Use of Ferrocene Derivatives as Linkers in Forming Metal Organic Frameworks (MOFs): Synthesis, Structural Characterization and Properties

Amita Agrawal

A dissertation submitted for the partial fulfillment of
BS-MS dual degree in Science

Indian Institute of Science Education and Research Mohali
May 2012

Certificate of Examination

This is to certify that the dissertation titled "Use of Ferrocene Derivatives in Forming Metal Organic Frameworks (MOFs): Synthesis, Structural Characterization and Properties" submitted by Ms. Amita Agrawal (Reg. No. MS07003) for the partial fulfillment of BS-MS dual degree programme of the Institute has been examined by the thesis committee members duly appointed by the Institute. The committee finds the work done by the candidate satisfactory and recommends that the thesis be accepted.

Prof. Ramesh Kapoor (Member)	Prof. K. S. Viswanathan (Member)	Dr. Sanjay Mandal (Convener & Supervisor)

Dated: May 4, 2012

Declaration

The work presented in this dissertation has been carried out by me under the guidance of Dr. Sanjay Mandal at the Indian Institute of Science Education and Research Mohali. This work has not been submitted in part or in full for a degree, a diploma, or a fellowship to any other university or institute. Whenever contributions of others are involved, every effort is made to indicate this clearly, with due acknowledgement of collaborative research and discussions. This thesis is a bonafide record of original work done by me and all sources listed within have been detailed in the bibliography.

Amita Agrawal
Dated: May 4, 2012

In my capacity as the supervisor of the candidate's project work, I certify that the above statements by the candidate are true to the best of my knowledge.

Dr. Sanjay Mandal
Dated: May 4, 2012

Acknowledgements

I express my sincere gratitude towards my project supervisor, Dr. Sanjay Mandal for his keen supervision and valuable advice. I thank him for the time he has spent discussing the problems and the results in and out of chemistry. This one year experience gave me an opportunity to learn not just chemistry and lab techniques from him but also values in life.

I am grateful to Prof. N Sathyamurthy for the motivation he provided whenever I felt low. I am thankful to all my chemistry teachers, Prof. Ramesh Kapoor, Dr. Sanjay Singh, Dr. Angshuman R. Choudhury, Dr. Ramesh Ramachandran, Dr. S. A. Babu, Dr. R. Vijaya Anand, Dr. Samrat Ghosh, Dr. Vinayak Sinha and Dr. Santanu Pal, who guided me through the entire period of MS. I would also like to thank Prof. K. S. Viswanathan and Dr. Shama Sundar for their kind support.

I am highly indebted to Sadhika di for her timely assistance, guidance and personal care. This project would have been impossible without her. I am grateful to my colleagues Navnita and Ankita for providing lively work atmosphere and their support throughout this project. I am thankful to Neelam, Vinod, Bhupesh Bhaiya and Nirdosh for their technical assistance. I would like to thank Mangat Bhaiya and Bahadur Bhaiya for their assistance. I am also thankful to all my friends and classmates.

I am grateful to IISER Mohali for providing me the facilities to carry out thr research work reported here. My special thanks to the MHRD for the INSPIRE fellowship for the past five years.

Last but not the least, I would like to thank my family and God for making this project possible.

List of Figures

List of Schemes

List of Tables

Abbreviations

A	Absorbance
calc.	Calculated
Cp	Cyclopentadienyl
DSC	Differential Scanning Calorimetry
H_2FcDC	Ferrocenedicarboxylic acid
H_2FcDS	Ferrocenedisulphonic acid
FTIR	Fourier Transform Infra-red
MOFs	Metal Organic Frameworks
MW	Molecular Weight
Na_2FcDC	Sodium Ferrocenedicarboxylate
$(NH_4)_2$FcDS	Ammonium Ferrocenedisulphonate
PXRD	Powder X-ray Diffraction
RT	Room Temperature
SCXRD	Single Crystal X-ray Diffraction
TGA	Thermal Gravimetric analysis
T	Transmittance
UV-vis	Ultraviolet-visible

Contents

Abstract

Based on ferrocene derivatives as linkers, new metal organic frameworks (MOFs) with a general formula $[M_4(tpxn)_2(FcDC)_2(H_2O)_4]^{4+}$ (FcDC = 1,1′-ferrocenedicarboxylate; tpxn = tppn, tpbn, tppen where tppn = N,N′,N″,N‴-tetrakis-(2-pyridylmethyl)-1,3-diaminopropane, tpbn = N,N′,N″,N‴- tetrakis-(2-pyridylmethyl)-1,4-diaminobutane, tppen = N,N′,N″,N‴-tetrakis-(2-pyridylmethyl)-1,5-diaminopentane, M^{2+} = Cu^{2+} (**1**, **2,** **3**), Cd^{2+} (**4**), Co^{2+} (**6**) and Mn^{2+} (**7**)) are reported. These are heterometallic MOFs. When $Fe^{3+}$is chosen as the metal ion a homometallic MOF, $\{[Fe_2(\mu\text{-}O)(tpbn)(FcDC)](ClO_4)_2 \cdot 4H_2O\}_n$ (**5**), is the product. Use of 1,1′-ferrocene disulphonate (FcDS) as the linker provides $[Cu_2(tpbn)(FcDS)_2]_n \cdot 4CH_3CN \cdot 2H_2O$ (**8a**) and $\{[Fe_2(\mu\text{-}O)(tpbn)(FcDS)](ClO_4)_2 \cdot 4H_2O\}_n$ (**9**). All complexes were characterised by elemental analysis, FTIR spectroscopy, UV-visible spectroscopy, mass spectometry, thermal gravimetric analysis, differential scanning calorimetry, single crystal and powder X-ray diffractometry. **1**, **2**, **3**, **4**, **6** and **7** are found to be discrete rectangular MOFs, **9** is a 1D coordination polymer, **5** is a 2D coordination polymer while **8a** is a 2D MOF.

Chapter I

Introduction

For a wide variety of applications, design and development of new porous materials continue to be an active field of research. Organic polymers and inorganic zeolites are the major porous materials known in the literature.[1] The former type includes compounds with large molecular weights composed of organic repeat units that are connected by covalent bonds. Zeolites are hydrated aluminosilicates having microporous structures. Aluminophosphates also form an important class of inorganic porous materials. These have a huge industrial application as size based separators. In the past two decades a new class of porous materials known as metal organic frameworks (MOFs) has been developed which is based on the combination of organic and inorganic moieties forming extensive frameworks. MOFs have the advantage over the organic and inorganic porous materials as they are highly designable frameworks and completely regular shaped with high porosity.[1-2]

Initially, research in this area started with the effort to make zeolite type materials. The goal was on changing the metal centers involved in zeolites. Metals from the same group were used as the initial substitutes which proved effective, e.g., gallium and germanium effectively replaced aluminum and silicon, respectively. Aluminium phosphate based molecular sieves discovered in 1982 formed the first non-silicon based oxide networks.[1-2]

With a shift in focus to design porous materials combining organic and inorganic moieties, the field of MOFs was initiated by Hoskins and Robson.[3] Development of new synthetic methodologies and demonstration of structure-activity relationships for various applications, such as catalysis, gas adsorption, magnetism, luminescent materials, etc., are the current focus of this broadly interdisciplinary research field.[2]

Metal Organic Frameworks (MOFs)

MOFs are 1-, 2-, or 3-dimensional polymeric materials consisting of metal ions or metal ion clusters connected together by multi-atom organic ligands called linkers.[4] The metal ion is usually a transition metal ion which serves as a versatile connector as it offers a variety of coordination number on which the dimensionality of the MOF depends. A metal ion in combination with an ancillary ligand forms the metal ion cluster. It may also be called a secondary building unit (SBU).[5] A linker joins the various units of connectors to form a framework. Neutral and anionic organic ligands are the most widely used linkers though a few examples of cationic organic ligands are also known. Examples of neutral linkers are nitrogen based organic moieties, such as pyrazine, 4,4'-bipyridine. Anionic linkers are mostly oxygen based organic compounds, such as di-, tri-, tetra-, and hexacarboxylates.[6] Cationic linkers are based on N-aryl pyridinium and 4,4'-bipyridinium derivatives. The size and shape of the organic linkers determine the size and shape of the pores in the framework. The longer organic linkers allow the formation of much larger pores than what is accessible through single oxygen linkers (as in case of zeolites).[2]

The number of open sites on the connector (M) which depends on the denticity of the ancillary ligand determines the dimensionality of the MOF as shown in Figure 1.[7] For example, a 1D MOF which is simply a linear chain can be realized by the use of a Ag^{+} as the metal ion. Similarly, a tetradentate ligand on a six coordinated Mn^{2+} leaves two open sites thus giving 1D MOF. A tridentate ligand leaves three open sites and hence is suitable to form 2D MOF.[5]

MOFs have mainly four types of bonding interactions: (i) coordination bond (CB), (ii) coordination bond and hydrogen bond (CB + HB), (iii) coordination bond and other interactions, such as π-π (PP), CH-π (HP) interactions, and (iv) coordination bond and mixture of interactions (e.g., HB + PP). Coordination bond contribution increases the stability of MOFs.[2]

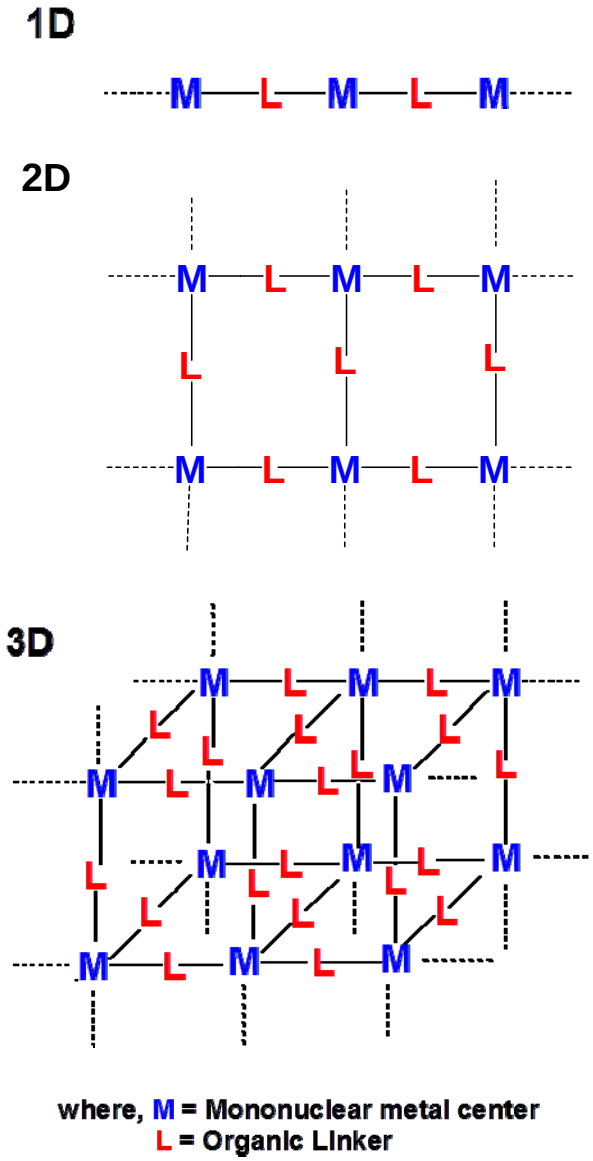

Figure 1. **Pictorial representation of 1D, 2D and 3D MOFs**.

One may confuse MOFs with supramolecules. There is a subtle difference between the two. Supramolecular chemistry involves investigation of molecular systems in which the most important feature is that the components are held together by weak interactions, not by covalent bonds while in case of MOFs, bonding is essentially covalent in nature. Figure 2 shows a 3D supramolecular assembly of 1D coordination polymer of (tmeda)Cu[Au(CN)$_2$]$_2$.[8]

The system is a one dimensional coordination polymer; its dimensionality increases to 3D owing to weak gold···gold interactions.

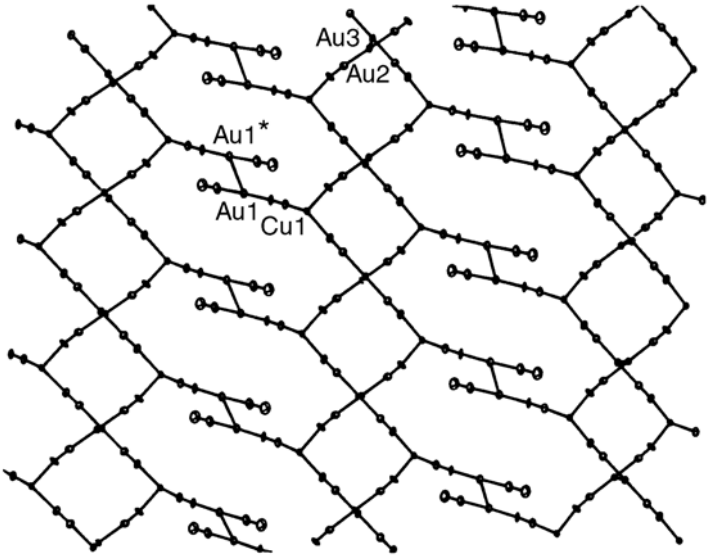

Figure 2. **3D supramolecular structure of (tmeda)Cu[Au(CN)$_2$]$_2$.**

Methods to Synthesize MOFs

Synthesis of MOFs is often associated with designing and engineering since MOFs can be made with a particular topology depending on their usage. Important parameters in the synthesis of MOFs involve understanding of the coordination environment of the metal ion, its interaction with the multi-atom organic linker and topologies possible from these interactions. Reaction conditions which would form these MOFs are also important.[9]

Traditionally, the typical one pot synthesis at room temperature has been used to make MOFs. In this method, a solution of metal ion and a solution of ligand are mixed together at room temperature and stirred for few hours to generate the MOF. The method has been embraced because of its simplicity. A drawback of this method is crystallizing the MOFs which often have solubility issues.

Various methods of crystallization have also been used to synthesize MOFs; these are based on the principle of concentration gradient which allows the formation of MOFs. These include slow diffusion of reactants into each other, solvent evaporation of a solution of reactants, and layering of solutions of reactants.

Over the years, many synthetic methods known in other fields [10-11] have also been applied to synthesize MOFs to give better quality products, reduce reaction times and enhance production scale. Prominent among them are solvothermal synthesis, microwave-assisted synthesis, electrochemical synthesis, sonochemical synthesis and mechanochemical synthesis.

Solvothermal reactions have been defined by Rabenau as the reactions taking place in closed vessels under autogenous pressure above the boiling point of the solvent.[12] In this method, all the reactants are mixed together with the solvent in a hydrothermal bomb and placed in a programmable oven under high temperature (120-180 ^{o}C) for a few days. Once the reaction time is over, the bomb is allowed to cool slowly over 10-12 hours affording crystals of MOFs directly. Here, the reaction times are long but the quality of MOF crystals obtained is good.

Microwave heating has been employed broadly as a means of accelerating the rate of chemical reactions. In presence of microwave-absorbing solvents, microwave heating causes the temperature to raise rapidly thus enhancing reaction rate. In this case direct interaction of the microwave radiation with the solvent/reactant occurs making it an energy-efficient method. Ni and Masel were the first to use microwave irradiation to synthesize MOFs; they made IRMOF-1 (also known as MOF-5), IRMOF−2 and IRMOF−3 with reaction times greatly reduced and products being microcrystalline.[9,13]

Sonochemical synthesis is yet another method that produces small MOF crystals with decreased reaction times. It employs the application of high-energy ultrasound waves to reaction mixtures. This does not involve any direct interaction between ultrasound and molecules as the wavelength of ultrasound is much larger than the molecular dimensions. In this method, regions of very high pressure and very low pressure are formed upon

sonochemical irradiation which results in the formation and collapse of bubbles in solution. This is called cavitation, which produces very high local temperatures (greater than 5000 K), resulting in extremely fast heating and cooling rates. Crystals of MOF-5 were obtained when the reaction was done with sonochemical irradiation in 1-methyl-2-pyrrolidinone (NMP). The product was similar in properties to the product synthesized via microwave and conventional heating.[9,14]

Anions, such as nitrate, perchlorate or chloride get incorporated into the framework of MOF during the synthesis which is a concern for their large-scale production. *Electrochemical synthesis* of MOFs was developed by BASF researchers in 2005 with the objective of excluding these anions. In electrochemical synthesis, a metal ion is the reactant instead of its salt. This is made possible by direct introduction of the metal ion into the reaction medium composed of the organic linker and a conducting salt through anodic dissolution.[9]

Another method of MOF synthesis is *mechanochemical synthesis*, also termed as solid-state synthesis. In this method, organic linker and the metal salt are ground together in a ball mill to produce the desired MOF. Pichon et al. first reported the synthesis of a copper-isonicotinic acid MOF using mechanochemical synthesis in 2006.[15] Solid-state syntheses do not involve the use of solvents and hence do away with the solubility issues of the reactants.[16] Hydrated metal salts enhance the reactivity due to the release of H_2O molecules which assists the grinding process. A modification in the method can be made by using very small amount of solvent. This is known as liquid-assisted grinding (LAG). Friscic and Fabian used LAG to obtain 1D, 2D, and 3D coordination polymers by varying the solvent added to a mixture of fumaric acid and ZnO.[17]

Applications of MOFs

MOFs are of interest not just because of their structural diversity but also because of plethora of their applications they have. They are useful in the fields of energy, environment, medicine, industry and host-guest studies. These can be used as storage materials, separators, sensors and catalysts.[2]

Gas absorption is one of the most important uses of MOFs.[18] Gases, such as methane and hydrogen, which are potential alternate fuel source, can be stored in the cavities of MOFs. Kitagawa et al. first reported the adsoption of methane in a Co (II) and 4,4'-bipyridine based MOF.[19] A lot of work has been done on the adsorption of hydrogen gas and it has been found that MOFs have great capacity to store high densities of the same.[20-21] .

Another important use of MOFs is *gas separation*. This is based on the dimensions of channels and pores of the MOF. Separation of CO_2 is a major area of interest from an environmental point of view. All the major economies of the world are putting enormous efforts to reduce carbon footprint. One way of reducing anthropogenic carbon emissions is size based capture and separation of CO_2 by using MOFs. Kim et al. showed selective uptake of CO_2 over N_2 or CH_4 by manganese (II) formate based MOF.[22]

Use of MOFs as *sensors* has also been demonstrated. An example of this is an MOF based on copper (II) and trimesic acid which detects the presence of organic aldehydes. When an organic substrate (aldehyde) replaces the coordinated water, a colour change occurs allowing the MOF to be used as a sensor.[23] Achmann et al. demonstrated the use of an iron-trimesic acid based MOF as humidity sensor. The main principle in this case is adsorption of water molecules from the environment causes a change in impedance of the MOF.[24]

Pores in MOFs can act as a site for catalysis and hence the use of MOFs as *catalysts* has been demonstrated. This reduces reaction times greatly and enhances product yields. Long et al. demonstrated the catalyses of cyanosilylation of aromatic aldehydes and the Mukaiyama-aldol reaction by a manganese (II) and benzene-tris(tetrazol-5-yl) based MOF.[25] Another example was reported by Gandara et al. wherein the MOF selectively catalysed the acetylation of aldehydes.[26]

MOFs have also contributed in the field of medicine as *drug delivery agents*. It is the porous nature and the well-defined channels of the MOFs that make the time controlled release of drug possible. Horcajada et al. reported the absorption of ibuprofen in the MOFs composed

of chromium and trimesic acid or terephthalic acid and subsequent time dependent release of the drug.[27] Importance of nitrous oxide as a biological signalling agent makes its release into the human body an attractive field of study. Morris et al. showed the adsorption of NO at room temperature and its release when exposed to moisture by cobalt (II) and nickel (II) based MOFs.[28]

Present Work

Dicyclopentadienyl iron (Cp_2Fe) was discovered by Kealy and Pauson in 1951.[29] The compound was given the name 'ferrocene' by Wilkinson, Rosenblum, Whiting and Woodward (1952), who had established its sandwich structure.[30-31] Since its discovery, ferrocene has interested chemists owing to its exceptional physical and chemical properties. It exhibits unusual stability for an organometallic compound based on an aromatic system. It decomposes above 470 ^{o}C. Interest sparked in the compound not only due to its stability but also because of its excellent redox properties. Reversible oxidation of ferrocene to ferrocenium cation can be achieved chemically and electrochemically. In addition, it shows interesting magnetic and optical properties.[32-35]

Chemically, ferrocene can be functionalized at either one cyclopentadienyl (Cp) ring or two Cp rings thus producing derivatives which can be useful in various fields. Two such ferrocene derivatives, 1,1′-ferrocene dicarboxylate (FcDC)[36] and 1,1′-ferrocene disulphonate (FcDS)[37] (Figure 3) have been employed as linkers in this study.

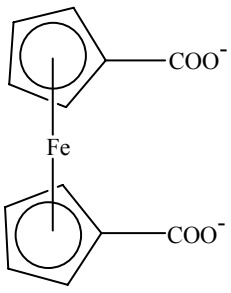

1,1′-Ferrocene dicarboxylate

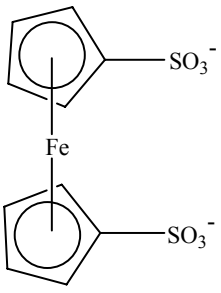

1,1′-Ferrocene disulphonate

Figure 3. **Anionic linkers used in the present work**.

Ferrocene based systems were chosen as the linker since ferrocene provides a robust backbone to the system and helps develop systems with interesting electrochemical, magnetic and optical properties. FcDC is a dicarboxylate and can bind to a metal ion centre in various ways[38-39] as shown in Figure 4. Sulphonates have been rarely employed as linkers because of their inability to coordinate strongly to the metal ion center. These are not even strong enough to displace solvent molecules from the coordination sphere of the transition metal ion.[40] This limits their use in the synthesis of MOFs.

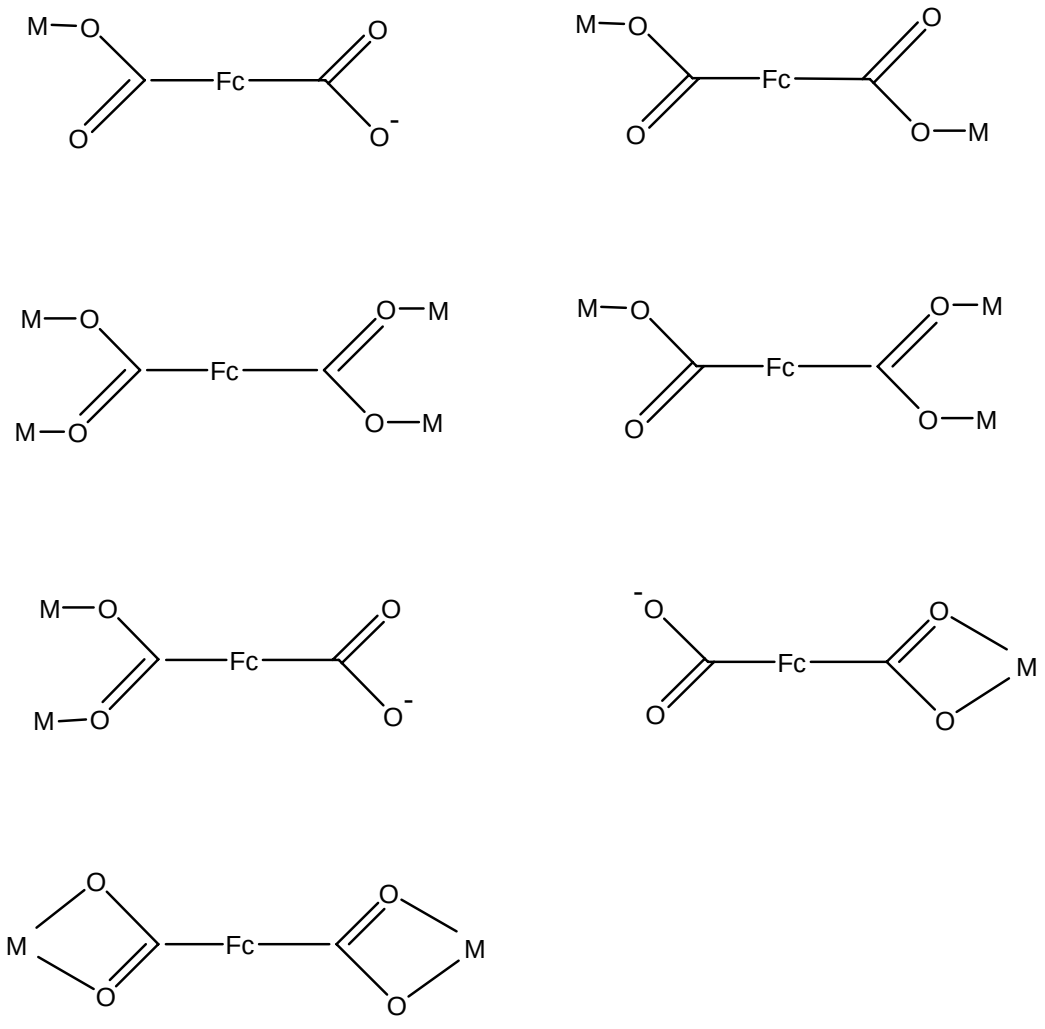

Figure 4. **Different binding modes of ferrocene dicarboxylate to a metal center**.

In the present work transition metal ions, such as Mn^{2+}, Fe^{3+}, Co^{2+}, Cu^{2+} and Cd^{2+}, were used. N,N′,N″,N‴-tetrakis-(2-pyridylmethyl)-1,4-diaminobutane (tpbn) and its variants N,N′,N″,N‴-tetrakis-(2-pyridylmethyl)-1,3-diaminopropane (tppn) and N,N′,N″,N‴-tetrakis-(2-pyridylmethyl)-1,5-diaminopentane (tppen) were used as the ancillary ligands (Figure 5)[41] which span between two metal ion centers, thus forming a metal cluster.

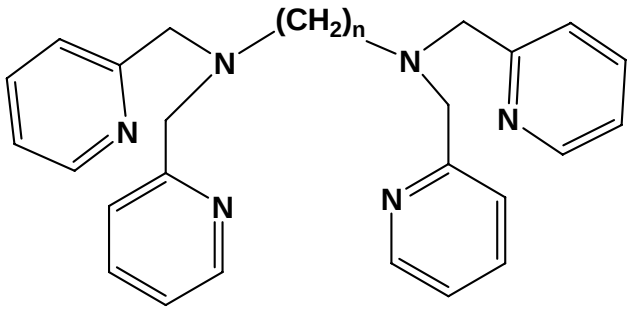

n=3, tppn; n=4, tpbn; n=5, tppen

Figure 5. **Ancillary ligands used in the present work**.

All complexes were characterised by elemental analysis, FTIR spectroscopy, UV-visible spectroscopy, mass spectometry, thermal gravimetric analysis, differential scanning calorimetry, single crystal and powder X-ray diffractometry.

Chapter II

Experimental Section

Materials and Methods

All chemicals and solvents used for synthesis were obtained from commercial sources and used as received without further purification. The ancillary ligands (tppn, tpbn, tppen) were obtained from Ms. Sadhika Khullar, PhD scholar, IISER Mohali. Elemental analysis (CHN) was carried out at Panjab University, Chandigarh and NIPER Mohali. Mass spectrometry, thermal gravimetric analysis (TGA) and differential scanning calorimetry (DSC) were done at NIPER, Mohali. FTIR spectra were collected for samples prepared as KBr pellets in the 400-4000 cm^{-1} range on a Perkin-Elmer Spectrum One spectrophotometer with a resolution of 4 cm^{-1}. UV-vis spectra were scanned between 400-800 nm on a Perkin-Elmer UV-Vis spectrometer with the bandwidth fixed at 1 nm. Single crystal and powder X-ray experiments were carried on a Bruker Kappa Apex II diffractometer and a Rigaku Ultima IV diffractometer, respectively, located in the X-ray facility of IISER Mohali.

Caution! Perchlorates were used as the metal salts in this study. Since these are explosive, proper care should be taken while handling the metal salts.

Synthesis

1,1′-Ferrocene Dicarboxylic acid [H_2FcDC]: A solution of ferrocene (1 g, 5.38 mmol) in dry hexane was added to n-butyllithium (8.4 mL, 13.45 mmol) and tetramethylethylenediamine (2.02 mL, 13.45 mmol) solution and stirred for 6 hours at room temperature (25 ºC) under dinitrogen. Dry ice was added to the above solution and stirred for 14 hours under dinitrogen. The solution was then filtered and washed with cold diethylether to collect the lithium salts of ferrocene dicarboxylic acid and ferrocene monocarboxylic acid. After redissolving the lithium salts in minimum amount of water, conc. hydrochloric acid

was added dropwise to it until no further precipitation occurred. A mixture of ferrocene dicarboxylic acid and ferrocene monocarboxylic acid was isolated via filtration followed by washing with water. The solid product (ferrocene dicaboxylic acid and ferrocene monocarboxylic acid) was dissolved in toluene. Ferrocene dicarboxylic acid was collected via filtration leaving ferrocene monocarboxylic acid in toluene. Yield: 86%. FTIR of H_2FcDC (KBr, cm^{-1}): $\nu_{C=O}$, antisymmetric 1685 (vs), $\nu_{C=O}$, symmetric 1301 (s). Na_2FcDC was prepared by treating the acid with 2 equivalents of NaOH in water. FTIR of Na_2FcDC (KBr, cm^{-1}): $\nu_{C=O}$, antisymmetric 1564 (vs) and $\nu_{C=O}$, symmetric 1398 (s).

1,1′-Ammonium Ferrocene Disulphonate [$(NH_4)_2FcDS$]: A solution of ferrocene (1g, 5.38 mmol) in acetic anhydride (10 mL) was taken in a 25 mL round bottom flask. Conc. H_2SO_4 was added dropwise (1.76 g, 18 mmol) to the above solution and the reaction mixture was allowed to stir for 24 hours at room temperature. After stirring was over, the reaction mixture was filtered using a sintered G-4 crucible. The dark green solid thus obtained was dissolved in water and 8 mL ammonia (25 wt %) was added to make it alkaline (pH = 10). Upon evaporation under vacuum, a dark brown solid was obtained. It was dissolved in ethanol and filtered. Addition of toluene to the filtrate yielded bright yellow crystals of ammonium ferrocene disulphonate. Yield: 65%. FTIR (KBr, cm^{-1}): $\nu_{S=O}$, antisymmetric 1423 (m), $\nu_{S=O}$, symmetric 1181 (vs), ν_{S-O}, 1054 (s).

General Procedure for Synthesis of Compounds with H_2FcDC

In a round bottom flask, an aqueous solution (3 mL) of Na_2FcDC [FcDC (34.2 mg, 0.125 mol) and NaOH (10 mg, 0.25 mol)] was added to methanolic solution (7 mL) of the metal salt (0.250 mol) and tpxn (0.125 mol). The resulting reaction mixture was stirred for 2 hours at room temperature. The solid product obtained was collected on a crucible via filtration, washed with methanol, and vacuum dried. In few cases KOH was used as the base instead of NaOH because the former gave precipitate and it was easy to remove the side product formed in case the product was obtained as filtrate.

$[Cu_4(tppn)_2(FcDC)_2(H_2O)_4](ClO_4)_4 \cdot 2H_2O$ (1): $Cu(ClO_4)_2 \cdot 6H_2O$ was used as the metal salt with tppn as the ancillary ligand. Green solid was obtained. Yield: 48%. Elemental analysis for $C_{78}H_{88}N_{12}O_{28}Cl_4Fe_2Cu_4$ (MW = 2144.38); calc.: C, 42.94 %, H, 4.07 %, N, 7.71 %;

found: C, 43.1 %, H, 3.7 %, N, 7.5 %. FTIR (KBr, cm^{-1}): 1611 (m), 1552 (m), 1470 (s), 1382 (m), 1092 (vs), 766 (m), 623 (m).

$[Cu_4(tpbn)_2(FcDC)_2(H_2O)_4](ClO_4)_4 \cdot 6H_2O$ (2): $Cu(ClO_4)_2 \cdot 6H_2O$ was used as the metal salt with tpbn as the ancillary ligand. Green solid was obtained. Yield: 63%. Elemental analysis for $C_{80}H_{100}N_{12}O_{34}Cl_4Fe_2Cu_4$ (MW = 2281.62); calc.: C, 42.11 %, H, 4.43 %, N, 7.37 %; found: C, 42.10 %, H, 4.00 %, N, 7.30 %. FTIR (KBr, cm^{-1}): 1610 (s), 1560(s), 1469 (s), 1383 (s), 1096 (vs), 768 (m), 623 (m).

$[Cu_4(tppen)_2(FcDC)_2(H_2O)_4](ClO_4)_4 \cdot 6H_2O$ (3): $Cu(ClO_4)_2 \cdot 6H_2O$ was used as the metal salt and tppen as the ancillary ligand. In this case KOH was used as a base. Green solid was obtained. Yield: 50%. Elemental analysis for $C_{82}H_{104}N_{12}O_{42}Cl_6Fe_2K_2Cu_4$ (MW = 2585.22); calc.: C, 38.06 %, H, 4.02 %, N, 6.49 %; found: C, 38.3 %, H, 3.6 %, N, 6.2 %. FTIR (KBr, cm^{-1}): 1611 (m), 1559 (s), 1466 (s), 1384 (m), 1098 (vs), 771 (m), 624 (m).

$[Cd_4(tpbn)_2(FcDC)_2(H_2O)_4](ClO_4)_4$ (4): $Cd(ClO_4)_2 \cdot 6H_2O$ was used as the metal salt with tpbn as the ancillary ligand. Light brown solid was obtained. Yield: 56%. Elemental analysis for $C_{80}H_{88}N_{12}O_{28}Cl_4Fe_2Cd_4$ (MW = 2368.94); calc.: C, 40.56 %, H, 3.75 %, N, 7.10 %; found: C, 43.90 %, H, 4.22 %, N, 7.98 %. FTIR (KBr, cm^{-1}): 1603 (m), 1551 (m), 1477 (s), 1387 (m), 1094 (vs), 767 (m), 626 (m).

$\{[Fe_2(\mu\text{-}O)(tpbn)(FcDC)](ClO_4)_2 \cdot 2H_2O\}_n$ (5): $Fe(ClO_4)_3 \cdot 6H_2O$ was used as the metal salt with tpbn as the ancillary ligand. Dark brown solid was obtained. Yield: 66%. Elemental analysis for $C_{40}H_{44}N_6O_{15}Cl_2Fe_3$ (MW = 1087.35): calc.: C, 44.17 %, H, 3.53 %, N, 7.48 %; found: C, 43.91 %, H, 3.82 %, N, 7.48 %. FTIR (KBr, cm^{-1}): 1607 (m), 1530 (m), 1477 (s), 1387 (m), 1095 (vs), 770 (m), 623 (m).

$[Co_4(tpbn)_2(FcDC)_2(H_2O)_4](ClO_4)_4 \cdot 4H_2O \cdot 1.5KClO_4$ (6): $Co(ClO_4)_2 \cdot 6H_2O$ was used as the metal salt with tpbn as the ancillary ligand. The product was obtained as reddish brown filtrate which was evaporated to dryness under vacuum to yield dark reddish brown solid. Yield (crude product): 85%. Elemental analysis for $C_{80}H_{92}N_{12}O_{38}Cl_{5.5}Fe_2Co_4K_{1.5}$ (MW = 2434.75); calc.: C, 39.4 %, H, 3.98 %, N, 6.91 %; found: C, 39.26 %, H, 4.09 %, N, 7.84 %. FTIR (KBr, cm^{-1}): 1608 (m), 1566 (m), 1483 (s), 1389 (m), 1096 (vs), 767 (m), 624 (m).

$[Mn_4(tpbn)_2(FcDC)_2(H_2O)_4](ClO_4)_4 \cdot KClO_4$ (7): $Mn(ClO_4)_2 \cdot 6H_2O$ was used as the metal salt with tpbn as the ancillary ligand. Here, KOH was used as a base. Light brown solid was obtained. Yield: 84%. Elemental analysis for $C_{80}H_{88}N_{12}O_{32}Cl_5Fe_2Mn_4K$ (MW = 2277.50); calc.: C, 42.15 %, H, 3.86 %, N, 7.38 %; found: C, 41.47 %, H, 3.77 %, N, 7.12 %. FTIR (KBr, cm^{-1}): 1604 (m), 1556 (m), 1480 (s), 1387 (m), 1096 (vs), 766 (m), 624 (m).

General Procedure for Synthesis of Compounds with $(NH_4)_2FcDS$

In a 25 mL round bottom flask, $(NH_4)_2FcDS$ (95 mg, 0.25mol) was added to methanolic solution (10 mL) of the metal salt (0.250 mol) and tpbn (57 mg, 0.125 mol). The resulting reaction mixture was stirred for 2 hours at room temperature. The solid thus obtained was collected on a crucible via filtration, washed with methanol and vacuum dried.

$[Cu_2(tpbn)(FcDS)_2]_n \cdot n\{[Cu_2(tpbn)(H_2O)_2](ClO_4)_4\}$(8): $Cu(ClO_4)_2 \cdot 6H_2O$ was used as the metal salt. Green solid was obtained. Yield: 81%. Elemental analysis for $C_{42}H_{42}N_6O_{15}S_2Cl_2Fe_1Cu_2$ (MW = 1140) considering 1:1 mixture of $[Cu_2(tpbn)(FcDS)_2]$ and $[Cu_2(tpbn)(H_2O)_2](ClO_4)_4$; calc.: C, 39.3 %, H, 3.67 %, N, 7.46 %, S, 5.05 %; found: C, 39.27 %, H, 4.02 %, N, 7.46 %, S, 6.70 %. FTIR (KBr, cm^{-1}): 1612 (m), 1448 (m), 1181 (s), 1099 (vs), 770 (m), 652 (m), 497 (m). Upon recrystallization of **8** in a mixture of acetonitrile and water provided single crystals of $\{[Cu_2(tpbn)(FcDS)_2] \cdot 4CH_3CN \cdot 2H_2O\}_n$ (**8a**) suitable for X-ray single crystal studies.

$\{[Fe_2(\mu\text{-}O)(tpbn)(FcDS)](ClO_4)_2 \cdot 4H_2O\}_n$ (9): $Fe(ClO_4)_3 \cdot 6H_2O$ was used as the metal salt. Brown solid was obtained. Yield: 75%. Elemental analysis for $C_{38}H_{48}N_6O_{19}S_2Cl_2Fe_3$ (MW = 1195.49): calc.: C, 38.18 %, H, 4.06 %, N, 7.03 %, S, 5.64 %; found: C, 38.23 %, H, 3.99 %, N, 6.78 %, S, 6.37 %. FTIR (KBr, cm^{-1}): 1611 (m), 1443 (m), 1185 (s), 1098 (vs), 769 (m), 649 (m), 500 (m).

Single Crystal X-ray Studies

Crystals suitable for the single crystal X-ray study were grown from the slow evaporation of solution of **8** in a 1:1 mixture of acetonitrile and water. Crystals of the compound were

transferred from mother liquor to mineral oil for manipulation, selection and mounting. A crystal was mounted on a thin glass fiber using feviglue and transferred to the goniometer head placed under a cold stream of nitrogen gas at 25 °C followed by slow cooling to the desired temperature (170 K). Crystals of appropriate dimensions were selected. Initial crystal evaluation and data collection were performed on a Kappa APEX II diffractometer equipped with a CCD detector (with the crystal-to-detector distance fixed at 60 mm) and sealed-tube monochromated Mo Kα radiation. The diffractometer was interfaced to a PC that controlled the crystal centering, unit cell determination, refinement of the cell parameters and data collection through the program APEX. For each sample, three sets of frames of data were collected with 0.30° steps in ω and an exposure time of 10 s within a randomly oriented region of reciprocal space surveyed to the extent of 1.3 hemispheres to a resolution of 0.85 Å. By using the program SAINT for the integration of the data, reflection profiles were fitted, and values of F^2 and $\sigma(F^2)$ for each reflection were obtained. Data were also corrected for Lorentz and polarization effects. The subroutine XPREP in the SHELXTL program was used for the processing of data that included determination of space group, application of an absorption correction, merging of data, and generation of files necessary for solution and refinement. All calculations were performed on a PC using the SHELXTL V 11.0 suite of programs. Crystallographic parameters and basic information pertaining to data collection and structure refinement are summarized in Table 13.

Powder X-ray Studies

PXRD data were recorded on a Rigaku Ultima IV diffractometer equipped with a 3 KW sealed tube Cu Kα X-ray radiation (generator power settings: 40 kV and 40 mA) and a DTex Ultra detector using parallel beam geometry (2.5° primary and secondary solar slits, 0.5° divergence slit with 10 mm height limit slit). Each sample grounded into a fine powder using a mortar and a pestle was placed on a glass sample holder that was placed on the sample rotation stage (120 rpm) attachment. The data were collected over an angle range 5° to 50° with a scanning speed of 1° per minute with 0.02° step with XRF reduction for metal complexes.

Chapter III

Results and Discussion

Synthesis

The aim of this study was to prepare homometallic and heterometallic MOFs. 1,1′-ferrocene dicarboxylate and 1,1′-ferrocene disulphonate were chosen as the linkers to achieve this goal. In addition, ferrocene backbone provides stability to the MOF as well as imparts interesting electrochemical, magnetic and optical properties. Connectors employed for this study were transition metal ions bridged by polypyridyl ancillary ligands; N,N′,N″,N‴-tetrakis-(2-pyridylmethyl)-1,4-diaminobutane (tpbn) was mainly used; in few cases its variants N,N′,N″,N‴-tetrakis-(2-pyridylmethyl)-1,3-diaminopropane (tppn) and N,N′,N″,N‴-tetrakis-(2-pyridylmethyl)-1,5-diaminopentane (tppen) were also used. Transition metal ions used were Mn^{2+}, Fe^{3+}, Co^{2+}, Cu^{2+} and Cd^{2+}.

H_2FcDC and $(NH_4)_2FcDS$ were prepared as reported in literature.[36-37] Schemes 1 and 2 show the steps involved in their synthesis, respectively. It may be pointed that H_2FcDS was further treated with ammonia to make the salt, $(NH_4)_2FcDS$, since the disulphonic acid is very moisture sensitive.

The method of preparation of the complexes was the conventional one pot synthesis at room temperature wherein solutions of all the reactants were mixed together and stirred for few hours to give the product via self-assembly of the starting material either as a solid or a solution.

For reactions with H_2FcDC (Scheme 3), the molar ratio of metal salt, H_2FcDC and tpxn was 2:1:1. Discrete heterometallic MOFs were obtained with general formula $[M_4(tpxn)_2(FcDC)_2(H_2O)_4]^{4+}$ for metal ions Cu^{2+} (**1**, **2, 3**), Cd^{2+} (**4**), Co^{2+} (**6**) and Mn^{2+} (**7**). In case of Fe^{3+} (**5**), homometallic polymeric 2D coordination polymer with formula $\{[Fe_2(\mu\text{-}O)(tpbn)(FcDC)](ClO_4)_2 \cdot 4H_2O\}_n$ was obtained (*vide infra*).

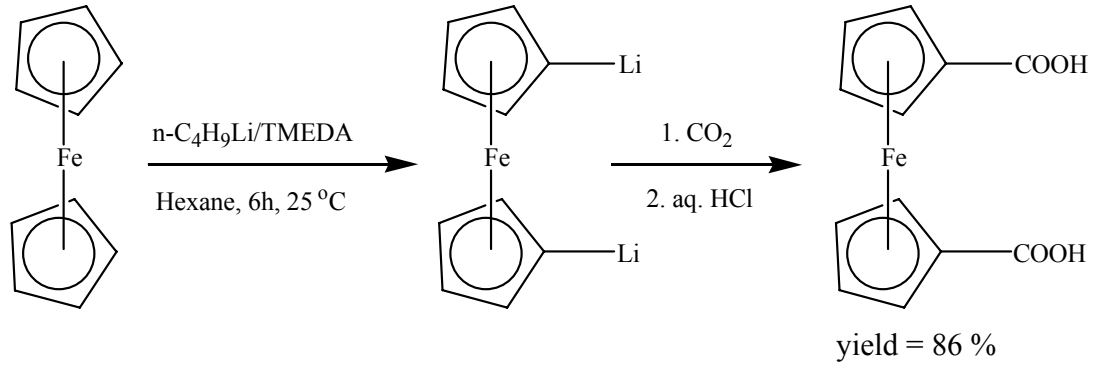

yield = 86 %

where TMEDA = tetramethylethylenediamine

Scheme 1. **Synthesis of H_2FcDS**.

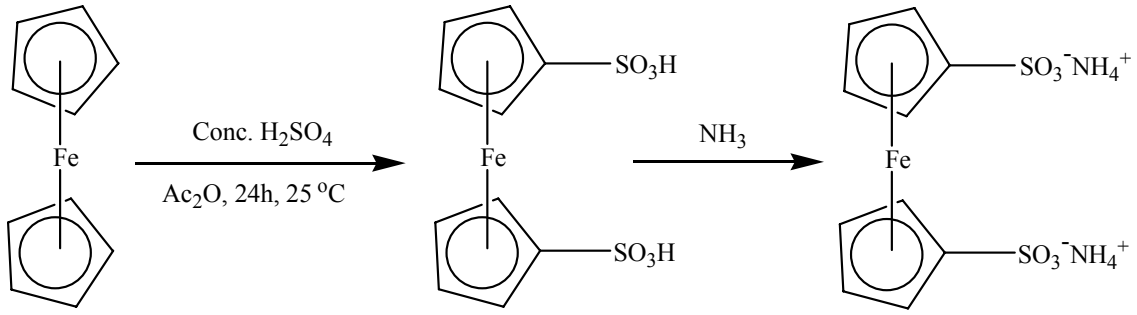

yield = 65 %

where Ac_2O = acetic anhydride

Scheme 2. **Synthesis of $(NH_4)_2FcDS$**.

MOFs **1**, **2**, **3** were obtained as green solids; **4** and **7** as light brown solids and **5** was a dark brown solid while **6** was obtained as filtrate which on evaporation under vacuum gave reddish-brown crystalline solid. MOFs **2**, **3** and **5** were soluble in mixture (4:1) of acetonitrile and water; **1** was soluble in water while **4** and **7** were soluble in dimethyl sulphoxide.

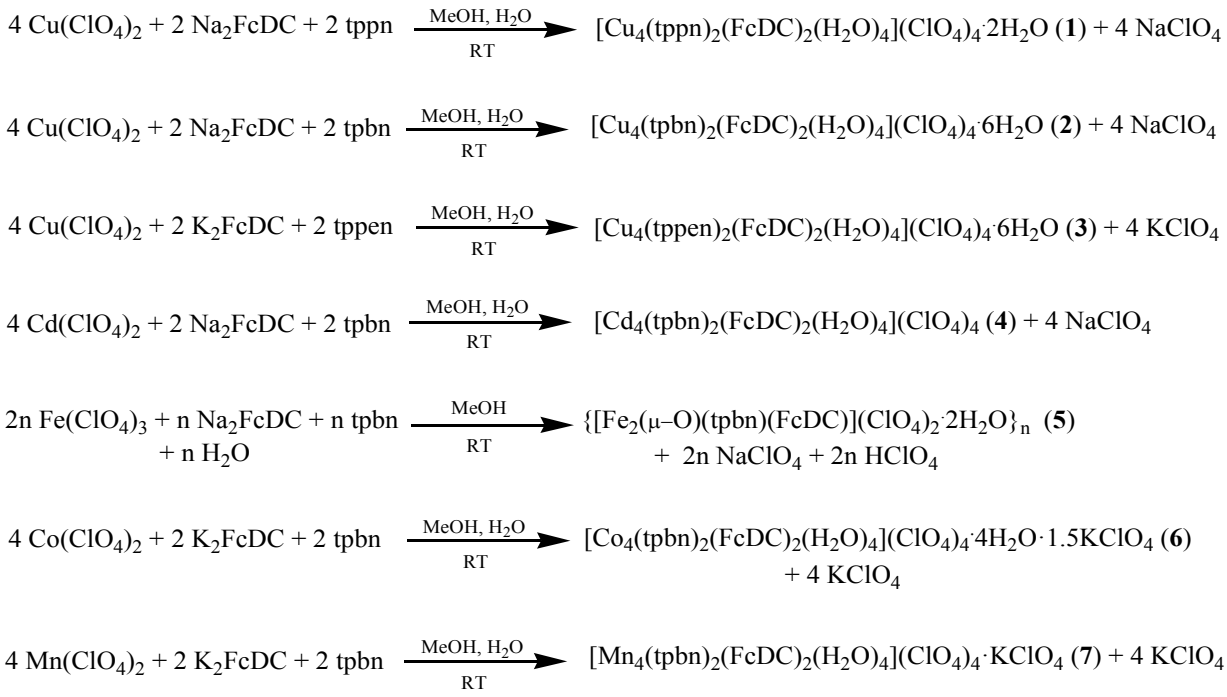

Scheme 3. **Synthesis of metal complexes with Na_2FcDC or K_2FcDC**.

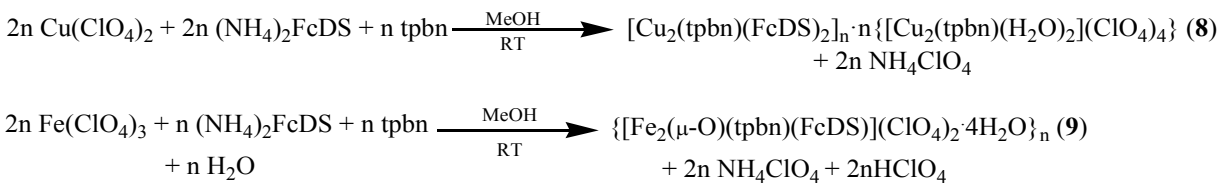

Scheme 4. **Synthesis of metal complexes with $(NH_4)_2FcDS$**.

For reactions with $(NH_4)_2$FcDS (Scheme 4), the molar ratio of metal salt, $(NH_4)_2$FcDS and tpbn was 2:2:1. 2D heterometallic MOF was obtained with formula $[Cu_2(tpbn)(FcDS)_2]_n$ for Cu^{2+} (**8a**) while a homometallic polymeric 1D coordination polymer with formula $\{[Fe_2(\mu\text{-}O)(tpbn)(FcDS)](ClO_4)_2 \cdot 4H_2O\}_n$ was obtained for Fe^{3+} (**9**). **8** was a green solid soluble in water while **9** was a dark brown solid soluble in hot acetonitrile.

In addition to the above complexes, attempts were made to get similar complexes for Ni^{2+}, Cr^{3+} and Pb^{2+} with FcDC and tpbn. In case of Ni^{2+}, the product was obtained as a filtrate. It gave brown crystalline solid on evaporation under vacuum. Elemental analysis, FTIR and mass spectral data were obtained but further work is needed to establish its correct formula. During reaction with Pb^{2+}, metal-tpbn complex formed initially. On addition of FcDC, tpbn was eliminated to give a Pb-FcDC complex (off-white shiny precipitate) as evident from the FTIR spectrum with peaks due to the carboxylate stretch but not the ligand peaks. On the other hand, the filtrate indicated peaks due to the ligand and not the carboxylate. For Cr^{3+}, the product was obtained as a filtrate. FTIR showed peaks for carboxylate as well as the ligand. Elemental analysis and mass spectral data were obtained but further work is needed to establish the correct formula.

Reactions with FcDS were also attempted with few other transition metal ions such as Cd^{2+}, Mn^{2+}, Ni^{2+} and Ag^{+}. In all cases, FcDS did not bind to the metal ion center based on the FTIR spectra data, only ligand and counter anion peaks were observed indicating the formation of metal-tpbn complex. In case of Ni^{2+}, the product was obtained as a filtrate which yielded crystals of two different colours, blue (Ni^{2+}-tpbn complex) and yellow (ammonium ferrocene disulphonate) upon recrystallization. The method of preparation of the complex was modified with the linker (FcDS) being added before the ancillary ligand (tpbn) to see if it got incorporated in the complex. The reactions were also tried by refluxing for a few days. In both cases, the results were the same; the metal-tpbn complexes formed. This shows poor binding nature of the sulphonates to these metal ions.

FTIR Spectroscopy

The IR spectra of all complexes recorded in the solid state show a broad band centered at 3400 cm^{-1} which is a characteristic feature for O-H stretching frequency of water molecules. Features centered around 1610 cm^{-1}, 1480 cm^{-1} and 770 cm^{-1} are indicative of the polypyridyl ligands. Peaks at 1095 cm^{-1} and 625 cm^{-1} are characteristic of ionic perchlorate.

For compounds with FcDC, strong carboxylate peaks centered around 1560 $cm^{-1}$and 1383 cm^{-1} are observed which are due to antisymmetric and symmetric carboxylate stretch, respectively except for **5**. For **5**, the antisymmetric stretch is shifted to 1530 cm^{-1}. This suggests that the carboxylate has a different binding mode for the iron complex. Strong bands around 1181 cm^{-1} and 1046 cm^{-1} are found in compounds with FcDS which are due to symmetric S=O stretch and S-O stretch respectively. Tables 1 and 2 show the stretching frequencies of carboxylates and sulphonates, respectively. FTIR spectra of all compounds are shown as below (Figures 6-14).

Table 1. **FTIR stretching frequencies for 1-7**.

S. No.	Compounds	$\nu_{Carboxylate}$ (cm^{-1})
1.	$[Cu_4(tppn)_2(FcDC)_2(H_2O)_4](ClO_4)_4 \cdot 2H_2O$	1552, 1382
2.	$[Cu_4(tpbn)_2(FcDC)_2(H_2O)_4](ClO_4)_4 \cdot 6H_2O$	1560, 1383
3.	$[Cu_4(tppen)_2(FcDC)_2(H_2O)_4](ClO_4)_4 \cdot 6H_2O$	1559, 1384
4.	$[Cd_4(tpbn)_2(FcDC)_2(H_2O)_4](ClO_4)_4$	1551, 1387
5.	$\{[Fe_2(\mu\text{-}O)(tpbn)(FcDC)](ClO_4)_2 \cdot 2H_2O\}_n$	1530, 1387
6.	$[Co_4(tpbn)_2(FcDC)_2(H_2O)_4](ClO_4)_4 \cdot 4H_2O \cdot 1.5KClO_4$	1566, 1389
7.	$[Mn_4(tpbn)_2(FcDC)_2(H_2O)_4](ClO_4)_4 \cdot KClO_4$	1556, 1387

Table 2. **FTIR stretching frequencies for 8 and 9**.

S. No.	Compounds	$\nu_{Sulphonate}$ (cm^{-1})
1.	$[Cu_2(tpbn)(FcDS)_2]_n \cdot n\{[Cu_2(tpbn)(H_2O)_2](ClO_4)_4\}$	1181, 1043
2.	$\{[Fe_2(\mu\text{-}O)(tpbn)(FcDS)](ClO_4)_2 \cdot 4H_2O\}_n$	1185, 1046

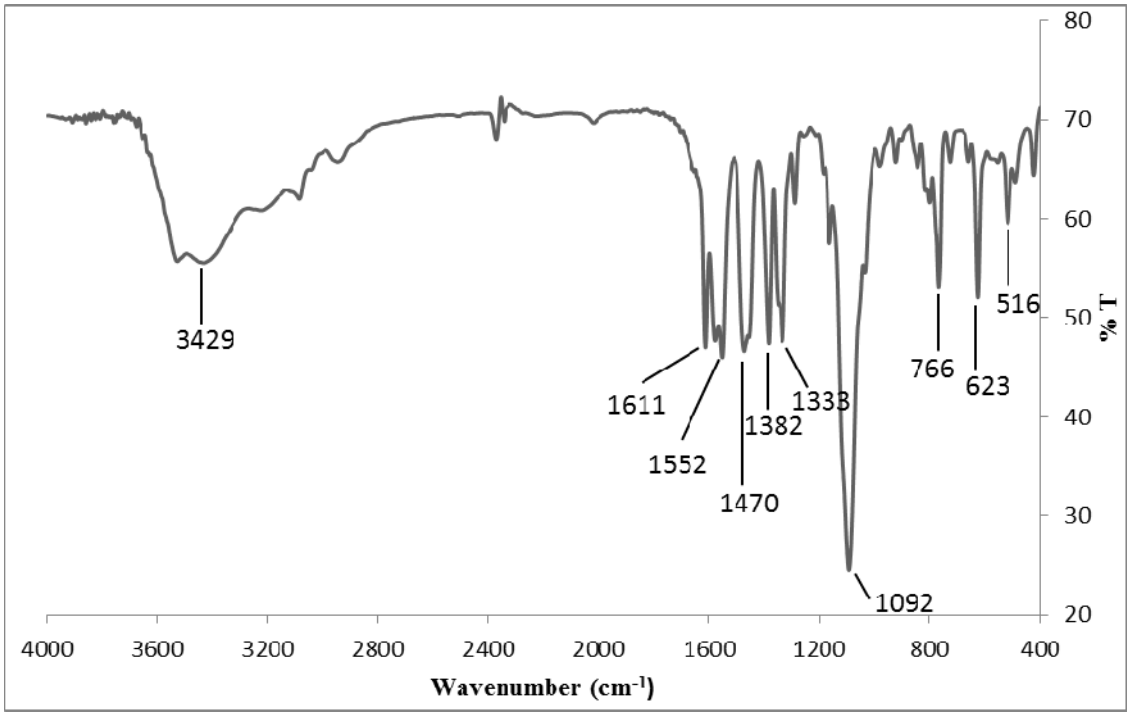

Figure 6. **FTIR spectrum for $[Cu_4(tppn)_2(FcDC)_2(H_2O)_4](ClO_4)_4 \cdot 2H_2O$ (1).**

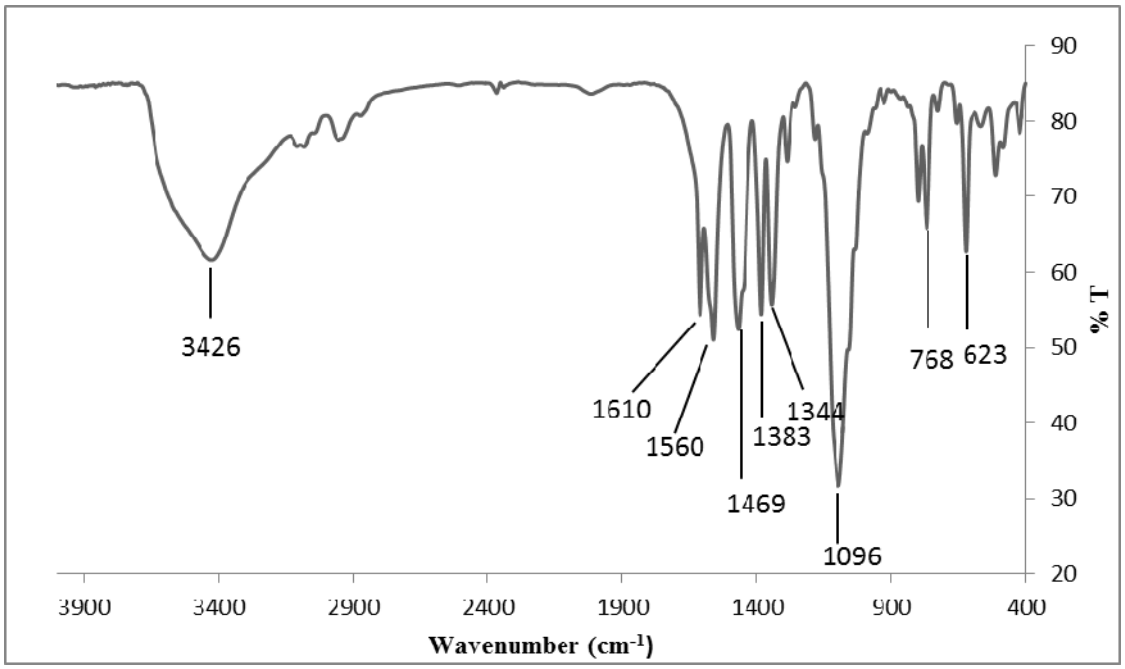

Figure 7. **FTIR spectrum for $[Cu_4(tpbn)_2(FcDC)_2(H_2O)_4](ClO_4)_4 \cdot 6H_2O$ (2).**

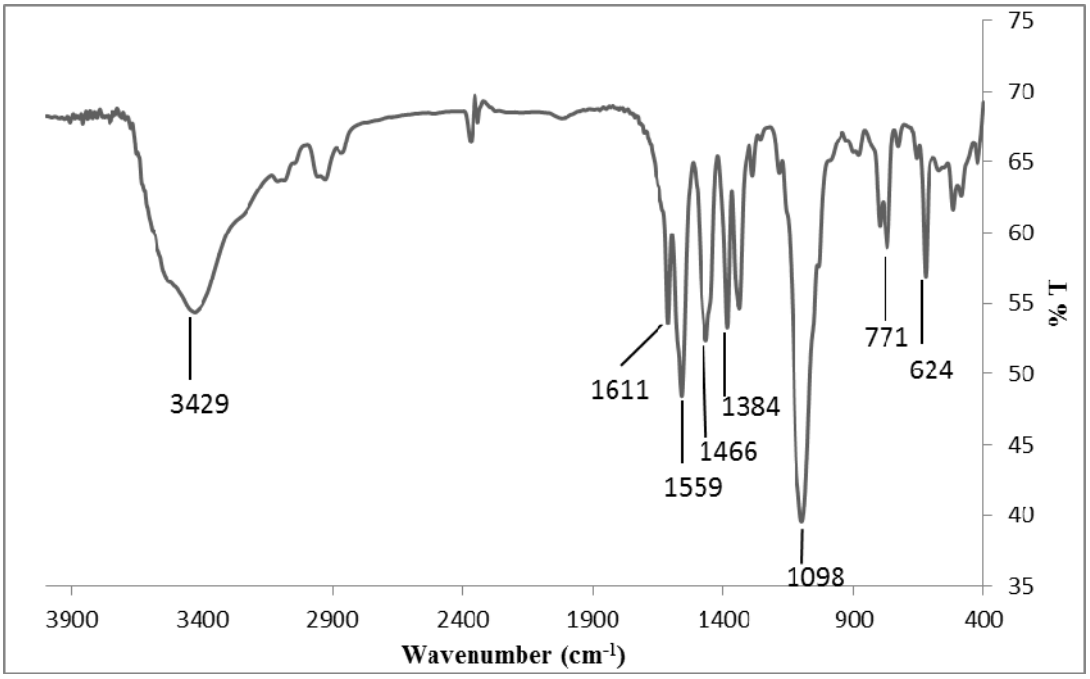

Figure 8. **FTIR spectrum for $[Cu_4(tppen)_2(FcDC)_2(H_2O)_4](ClO_4)_4 \cdot 6H_2O$ (3)**.

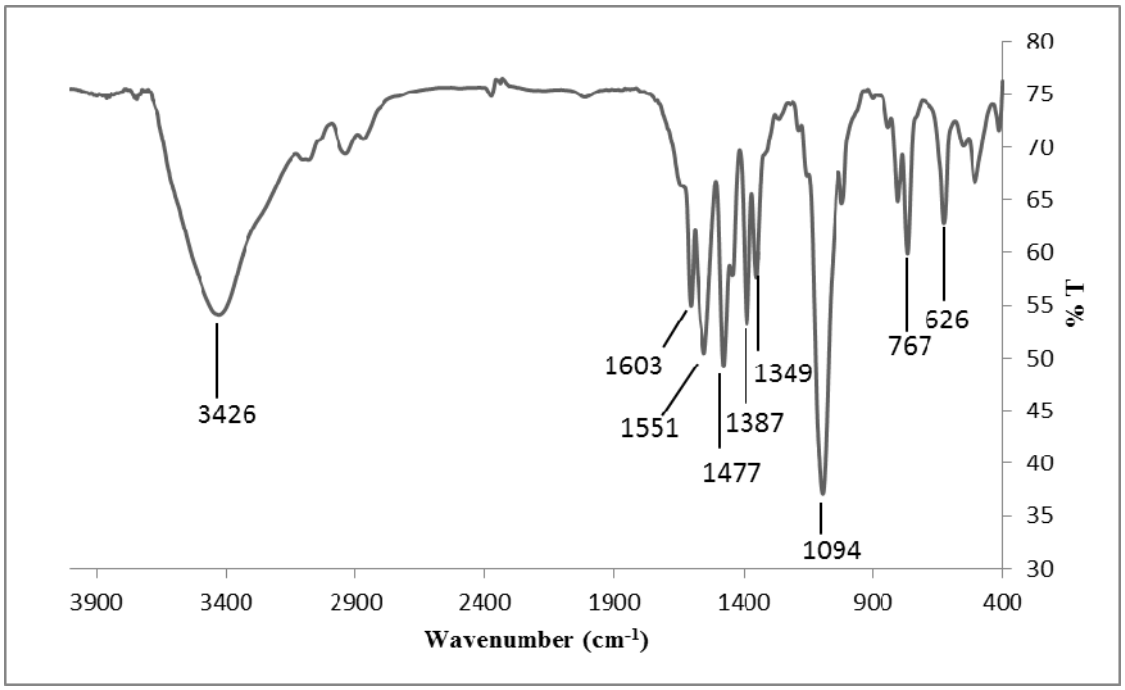

Figure 9. **FTIR spectrum for $[Cd_4(tpbn)_2(FcDC)_2(H_2O)_4](ClO_4)_4$ (4)**.

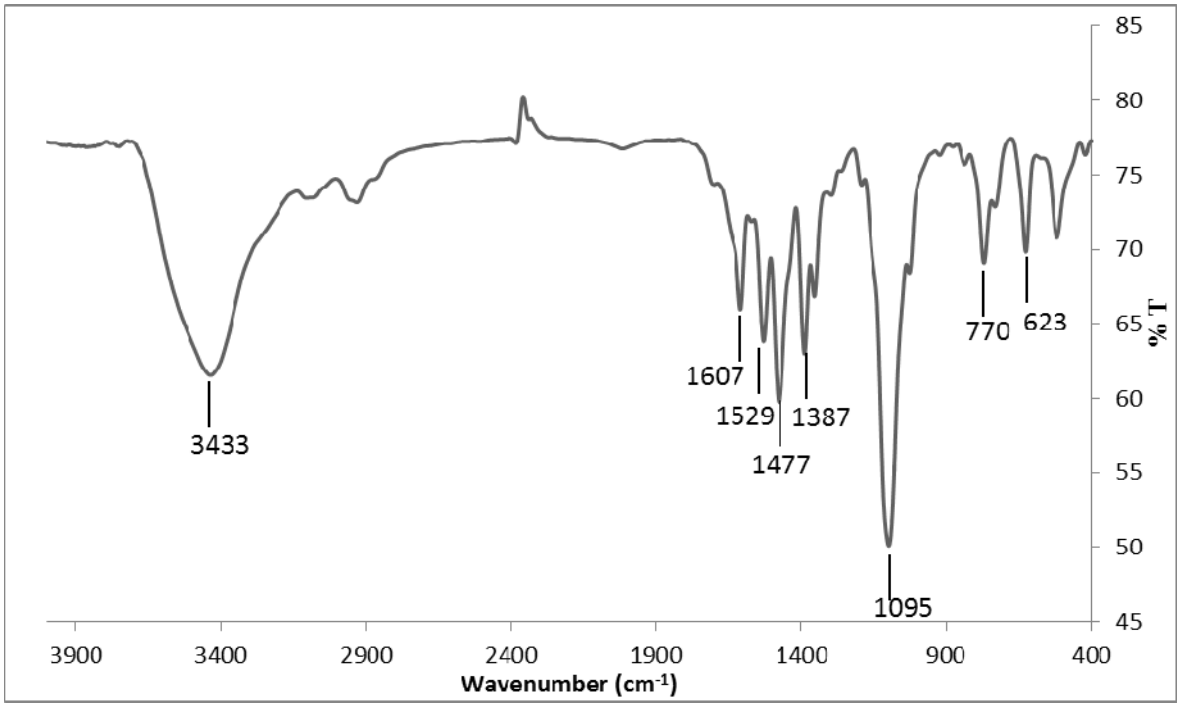

Figure 10. **FTIR spectrum for $\{[Fe_2(\mu\text{-}O)(tpbn)(FcDC)](ClO_4)_2 \cdot 2H_2O\}_n$ (5)**.

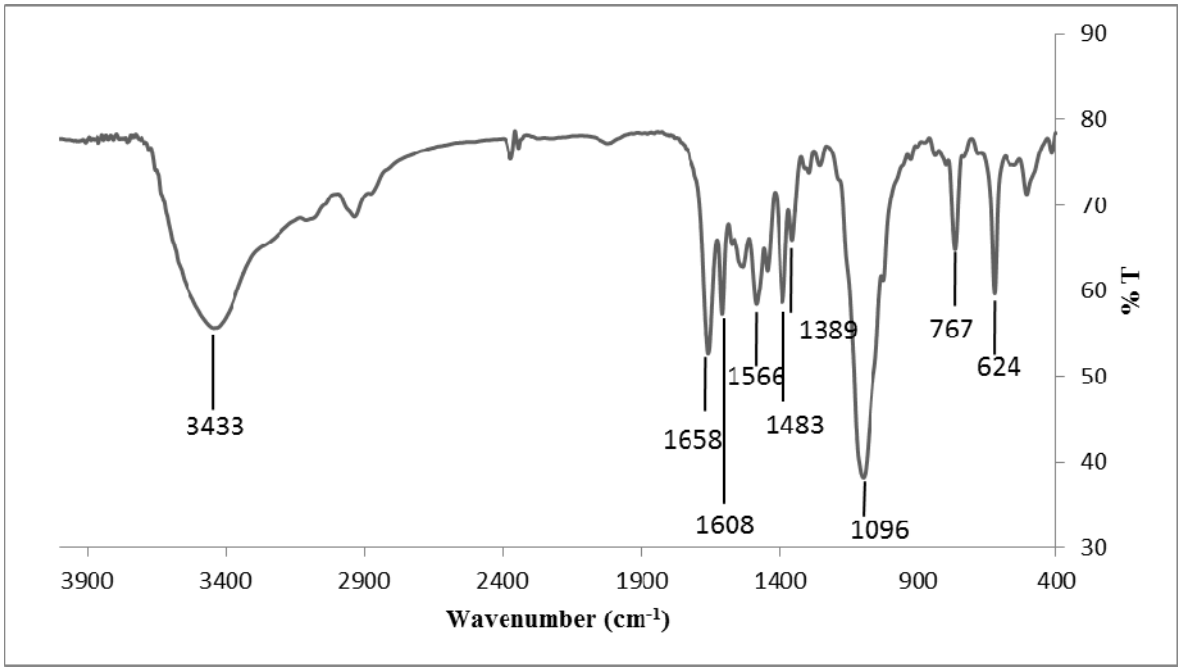

Figure 11. **FTIR spectrum for $[Co_4(tpbn)_2(FcDC)_2(H_2O)_4](ClO_4)_4 \cdot 4H_2O \cdot 1.5KClO_4$ (6)**.

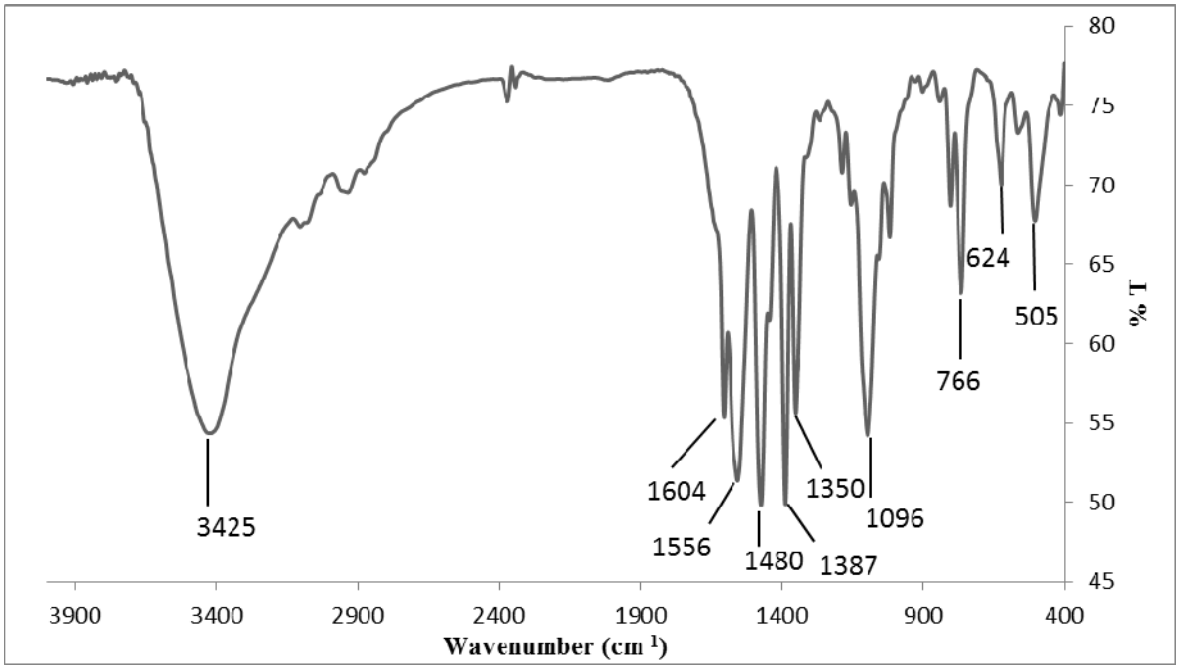

Figure 12. **FTIR spectrum for $[Mn_4(tpbn)_2(FcDC)_2(H_2O)_4](ClO_4)_4 \cdot KClO_4$ (7)**.

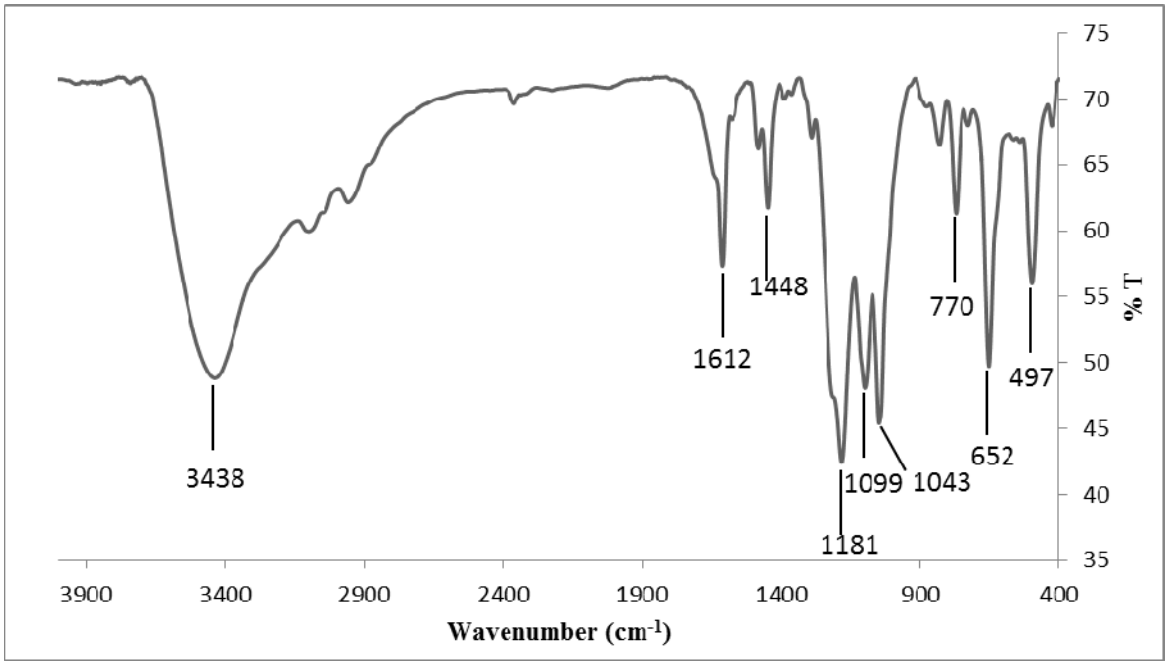

Figure 13. **FTIR spectrum for $[Cu_4(tpbn)(FcDS)_2]_n \cdot n\{[Cu_2(tpbn)(H_2O)_2](ClO_4)_4\}$ (8)**.

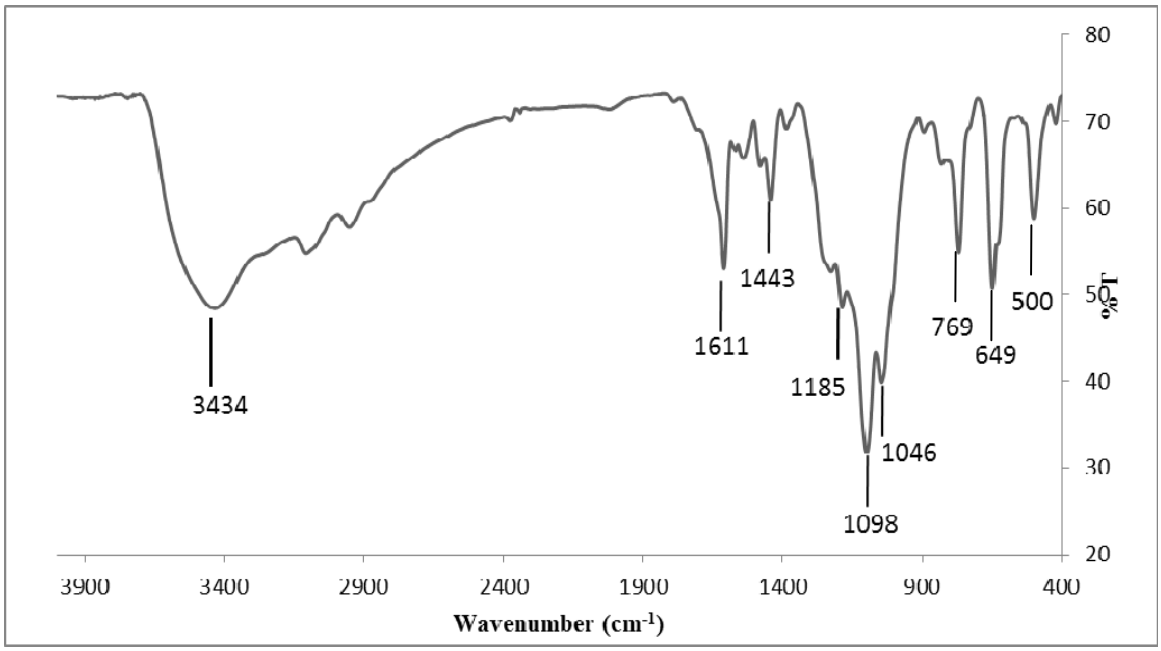

Figure 14. **FTIR spectrum for {[Fe_2(μ-O)(tpbn)(FcDS)](ClO_4)$_2$·4H_2O}$_n$ (9)**.

UV-visible Spectroscopy

All complexes and linkers prepared in this report were studied for their electronic transitions in the 400-800 nm range. λ_{max} for Na_2FcDC was observed at 445 nm while for $(NH_4)_2$FcDS, it was observed at 429 nm. In all complexes, a peak was found around 450 nm indicating the presence of linker. **1**, **2**, **3** and **8** showed an additional peak around 640 nm which is a characteristic of Cu^{2+}. In **5** and **9**, peaks were observed at 421 nm and 503 nm, which is a characteristic of Fe_2O core. Λ values for Na_2FcDC, $(NH_4)_2$FcDS and all compounds are summarized in Table 3. UV-vis spectra for Na_2FcDC, $(NH_4)_2$FcDS and all compounds were plotted between absorbance (A) and wavelength (λ) as shown in Figures 15-25 below.

Table 3. **Summary of UV-vis spectroscopic data for the metal complexes**.

S. No.	Compounds	λ values (nm)
1.	$[Cu_4(tppn)_2(FcDC)_2(H_2O)_4](ClO_4)_4 \cdot 2H_2O$	445, 636
2.	$[Cu_4(tpbn)_2(FcDC)_2(H_2O)_4](ClO_4)_4 \cdot 6H_2O$	448, 647
3.	$[Cu_4(tppen)_2(FcDC)_2(H_2O)_4](ClO_4)_4 \cdot 6H_2O$	452, 630
4.	$[Cd_4(tpbn)_2(FcDC)_2(H_2O)_4](ClO_4)_4$	433
5.	$\{[Fe_2(\mu\text{-}O)(tpbn)(FcDC)](ClO_4)_2 \cdot 2H_2O\}_n$	445, 503
6.	$[Co_4(tpbn)_2(FcDC)_2(H_2O)_4](ClO_4)_4 \cdot 4H_2O \cdot 1.5KClO_4$	450
7.	$[Mn_4(tpbn)_2(FcDC)_2(H_2O)_4](ClO_4)_4 \cdot KClO_4$	432
8.	$[Cu_2(tpbn)(FcDS)_2]_n \cdot n\{[Cu_2(tpbn)(H_2O)_2](ClO_4)_4\}$	446, 647
9.	$\{[Fe_2(\mu\text{-}O)(tpbn)(FcDS)](ClO_4)_2 \cdot 4H_2O\}_n$	421, 503

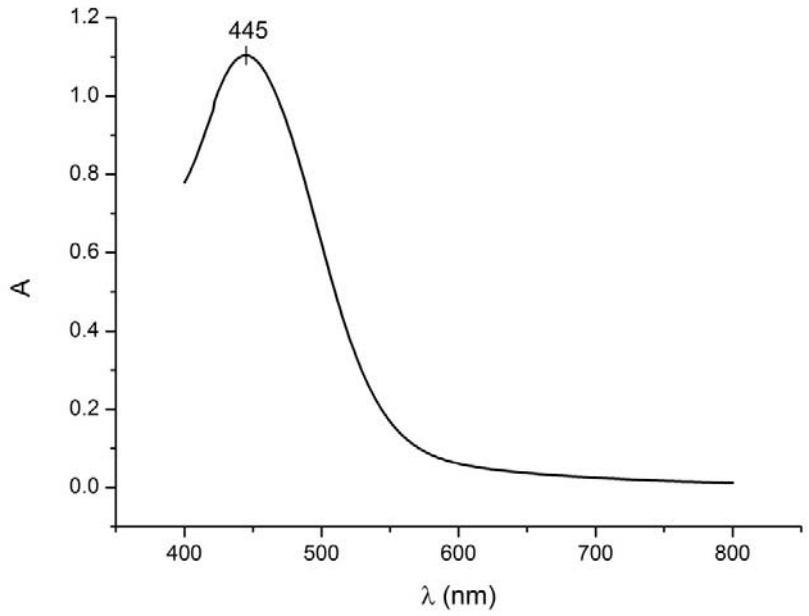

Figure 15. **UV-vis spectrum for Na_2FcDC**.

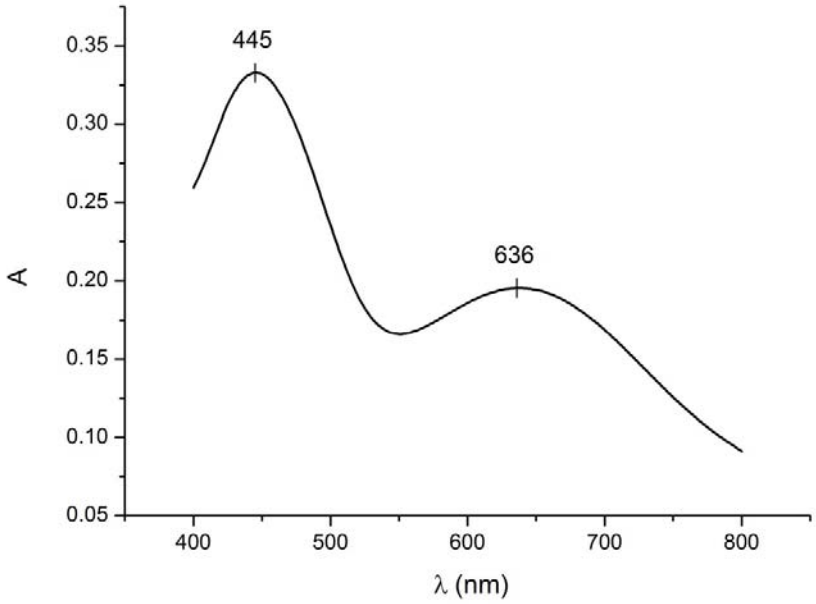

Figure 16. **UV-vis spectrum for 1**.

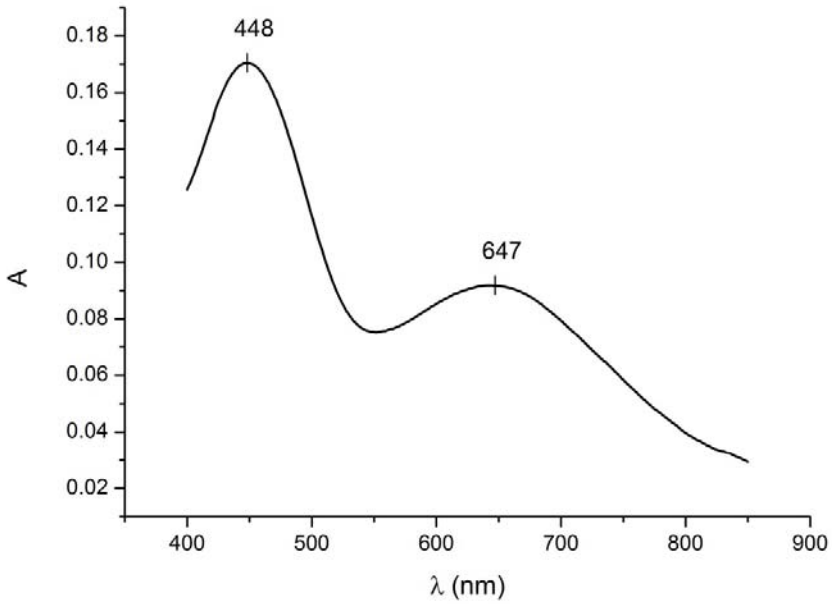

Figure 17. **UV-vis spectrum for 2**.

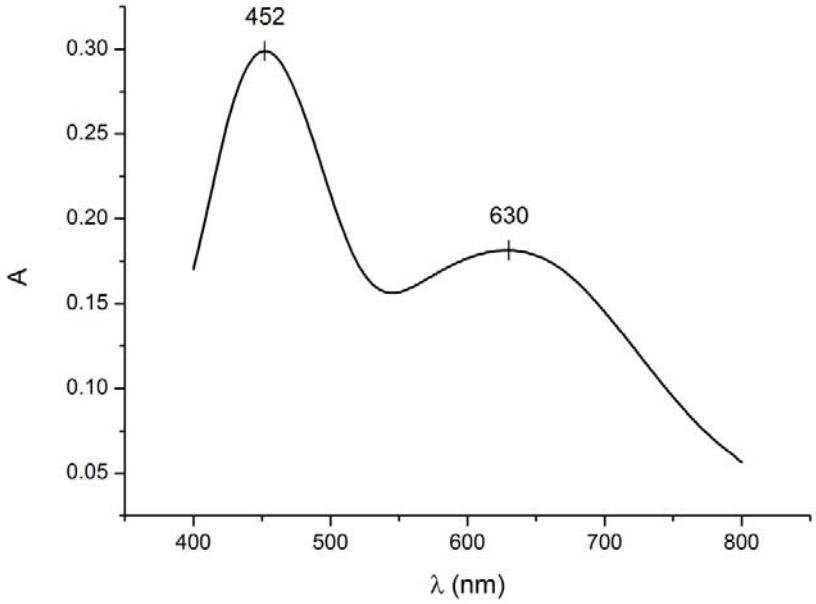

Figure 18. **UV-vis spectrum for 3**.

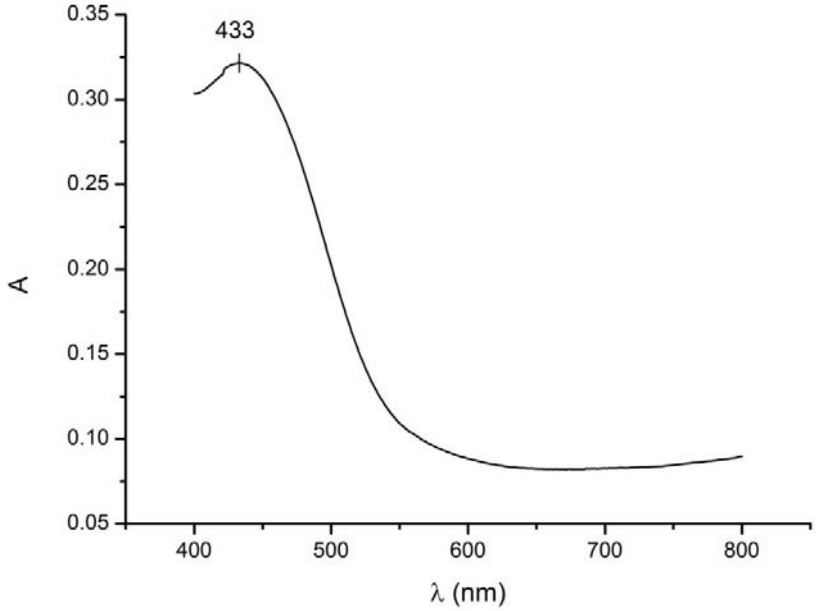

Figure 19. **UV-vis spectrum for 4**.

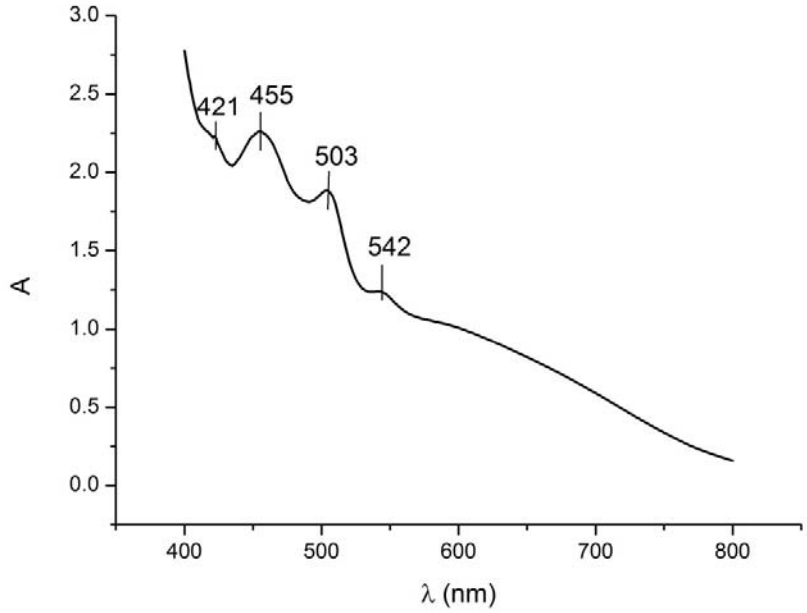

Figure 20. **UV-vis spectrum for 5**.

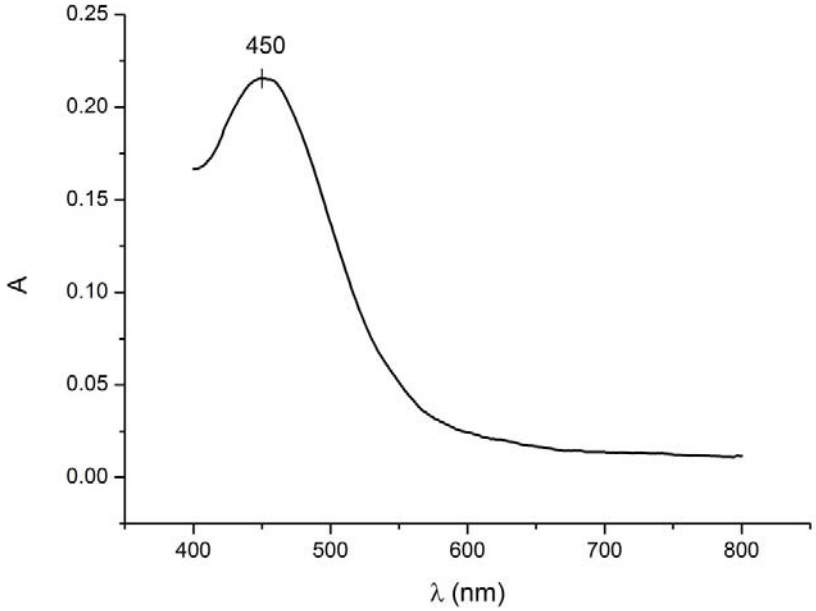

Figure 21. **UV-vis spectrum for 6**.

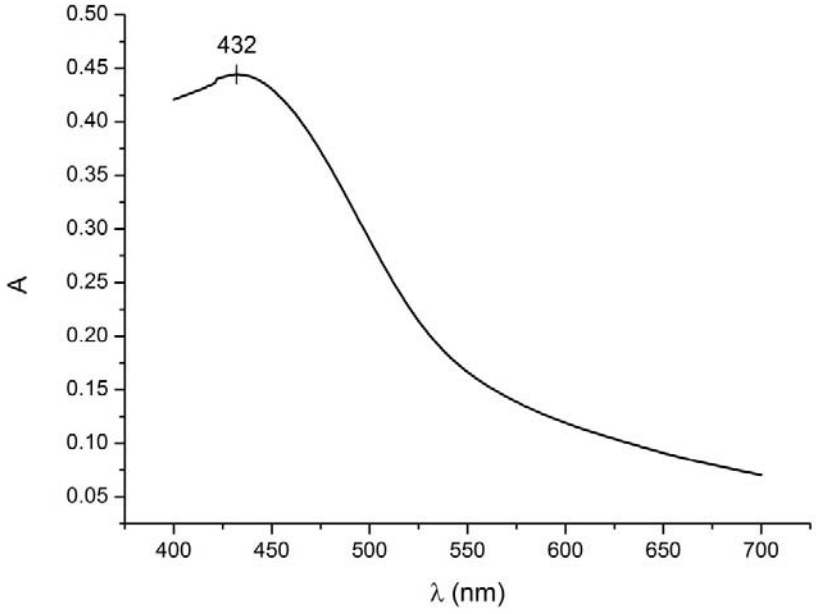

Figure 22. **UV-vis spectrum for 7**.

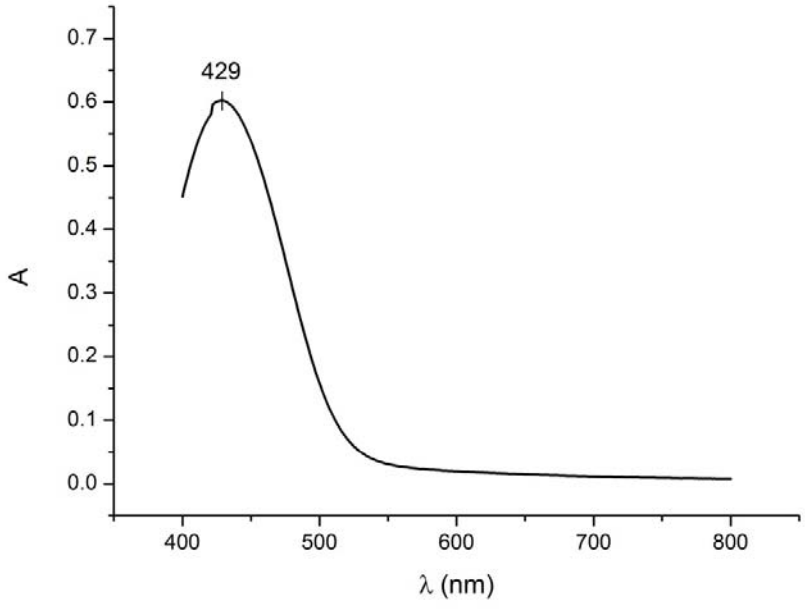

Figure 23. **UV-vis spectrum for $(NH_4)_2$FcDS**.

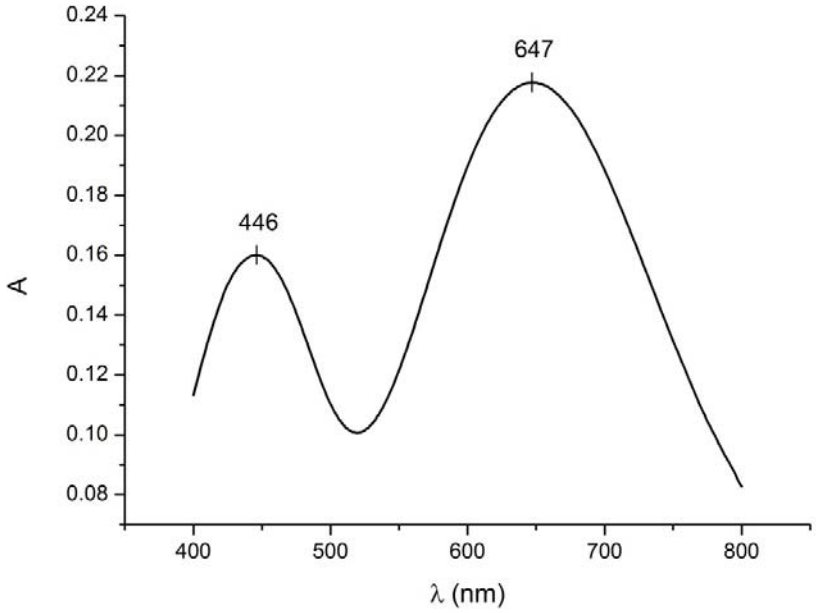

Figure 24. **UV-vis spectrum for 8**.

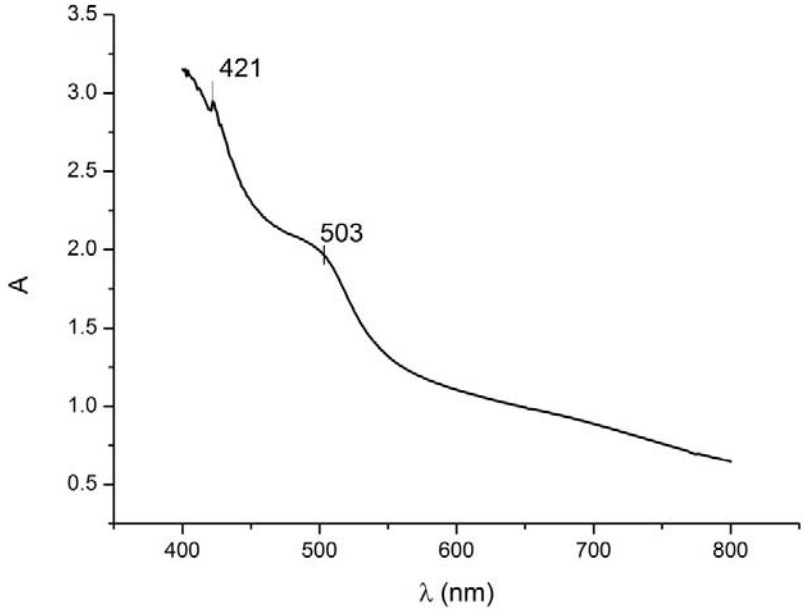

Figure 25. **UV-vis spectrum for 9**.

Mass Spectrometry

Mass spectrometry is a very useful technique for identifying the structure of compounds in solution depending on their fragmentation pattern. Electrospray Ionization Mass Spectrometry (ESI-MS) was done for all compounds in the molecular weight range 50-2000 in the positive mode. Two common peaks were observed in all the spectra: 227 and 453 which are due to protonated fragment of the tpbn molecule and protonated tpbn molecule, respectively. The fragmentation pattern for each compound is described in the tables below.

In a few cases, no peak was observed for monocationic species. This was due to the fact that the mass of these species exceeds 2000, which is out of the range of the instrument.

Table 4. **Mass spectral data for $[Cu_4(tppn)_2(FcDC)_2(H_2O)_4](ClO_4)_4 \cdot 2H_2O$ (MW = 2181.48)**.

S. No.	Molecular ion	m/z calc. (found)
1.	$\{[Cu_4(tppn)_2(FcDC)_2](ClO_4)_3\}^{1+}$	1973.74 (1973.13)
2.	$\{[Cu_4(tppn)_2(FcDC)_2](ClO_4)_2\}^{2+}$	937.14 (937.28)
3.	$\{[Cu_4(tppn)_2(FcDC)_2]ClO_4\}^{3+}$	591.61
4.	$[Cu_4(tppn)_2(FcDC)_2]^{4+}$	418.85 (419.44)

Table 5. **Mass spectral data for $[Cu_4(tpbn)_2(FcDC)_2(H_2O)_4](ClO_4)_4 \cdot 6H_2O$ (MW = 2281.62)**.

S. No.	Molecular ion	m/z calc. (found)
1.	$\{[Cu_4(tpbn)_2(FcDC)_2](ClO_4)_3\}^{1+}$	2001.79
2.	$\{[Cu_4(tpbn)_2(FcDC)_2](ClO_4)_2\}^{2+}$	951.17 (951.11)
3.	$\{[Cu_4(tpbn)_2(FcDC)_2]ClO_4\}^{3+}$	600.96
4.	$[Cu_4(tpbn)_2(FcDC)_2]^{4+}$	425.86 (425.37)

Table 6. **Mass spectral data for $[Cu_4(tppen)_2(FcDC)_2(H_2O)_4](ClO_4)_4 \cdot 6H_2O$ (MW = 2309.30)**.

S. No.	Molecular ion	m/z calc. (found)
1.	$\{[Cu_4(tppen)_2(FcDC)_2](ClO_4)_3\}^{1+}$	2029.85
2.	$\{[Cu_4(tppen)_2(FcDC)_2](ClO_4)_2\}^{2+}$	965.20 (965.39)
3.	$\{[Cu_4(tppen)_2(FcDC)_2]ClO_4\}^{3+}$	610.31
4.	$[Cu_4(tppen)_2(FcDC)_2]^{4+}$	432.87 (433.47)

Table 7. **Mass spectral data for $[Cd_4(tpbn)_2(FcDC)_2(H_2O)_4](ClO_4)_4$ (MW = 2368.72)**.

S. No.	Molecular ion	m/z calc. (found)
1.	$\{[Cd_4(tpbn)_2(FcDC)_2](ClO_4)_3\}^{1+}$	2197.25
2.	$\{[Cd_4(tpbn)_2(FcDC)_2](ClO_4)_2\}^{2+}$	1048.90 (1049.13)
3.	$\{[Cd_4(tpbn)_2(FcDC)_2]ClO_4\}^{3+}$	666.11 (665.23)
4.	$[Cd_4(tpbn)_2(FcDC)_2]^{4+}$	474.73

Table 8. **Mass spectral data for $\{[Fe_2(\mu\text{-}O)(tpbn)(FcDC)](ClO_4)_2 \cdot 2H_2O\}_n$ (MW = 1087.35)**.

S. No.	Molecular ion	m/z calc. (found)
1.	$\{[Fe_2(\mu\text{-}O)(tpbn)(FcDC)]ClO_4\}^{1+}$	951.77 (951.23)
2.	$[Fe_2(\mu\text{-}O)(tpbn)(FcDC)]^{2+}$	426.16 (426.36)

Table 9. **Mass spectral data for $[Co_4(tpbn)_2(FcDC)_2(H_2O)_4](ClO_4)_4 \cdot 4H_2O \cdot 1.5KClO_4$ (MW = 2434.75)**.

S. No.	Molecular ion	m/z calc. (found)
1.	$\{[Co_4(tpbn)_2(FcDC)_2](ClO_4)_3\}^{1+}$	1983.34 (1983.36)
2.	$\{[Co_4(tpbn)_2(FcDC)_2](ClO_4)_2\}^{2+}$	941.95 (941.32)
3.	$\{[Co_4(tpbn)_2(FcDC)_2]ClO_4\}^{3+}$	594.81
4.	$[Co_4(tpbn)_2(FcDC)_2]^{4+}$	421.25 (421.26)

Table 10. **Mass spectral data for $[Mn_4(tpbn)_2(FcDC)_2(H_2O)_4](ClO_4)_4 \cdot KClO_4$ (MW = 2277.5)**.

S. No.	Molecular ion	m/z calc. (found)
1.	$\{[Mn_4(tpbn)_2(FcDC)_2](ClO_4)_3\}^{1+}$	1967.36
2.	$\{[Mn_4(tpbn)_2(FcDC)_2](ClO_4)_2\}^{2+}$	933.96 (933.31)
3.	$\{[Mn_4(tpbn)_2(FcDC)_2]ClO_4\}^{3+}$	589.49
4.	$[Mn_4(tpbn)_2(FcDC)_2]^{4+}$	417.25 (417.45)

Table 11. **Mass spectral data for $\{[Cu_2(tpbn)(FcDS)_2] \cdot 4CH_3CN \cdot 2H_2O\}_n$ (MW = 1267.97)**.

S. No.	Molecular ion	m/z calc. (found)
1.	$[Cu_2(tpbn)(FcDS)]^{2+}$	461.91 (462.28)
2.	$[Cu_2(tpbn)]^{4+}$	144.92 (144.98)

Table 12. **Mass spectral data for $\{[Fe_2(\mu\text{-}O)(tpbn)(FcDS)](ClO_4)_2 \cdot 4H_2O\}_n$ (MW = 1195.49)**.

S. No.	Molecular ion	m/z calc. (found)
1.	$\{[Fe_2(\mu\text{-}O)(tpbn)(FcDS)]ClO_4\}^{1+}$	1023.88 (1022.96)
2.	$[Fe_2(\mu\text{-}O)(tpbn)(FcDS)]^{2+}$	462.21 (462.30)

Single Crystal X-ray Studies

{[Cu_2(tpbn)(FcDS)$_2$]·4CH_3CN·2H_2O}$_n$, 8a, crystallised in the monoclinic P system having the space group $P2_1/c$. It is a 2D heterometallic coordination polymer as shown in Figure 26. Each Cu^{2+} center is pentacoordinated with an N_3O_2 environment where 'N' belongs to the polypyridyl ligand, 'O' belongs to the sulphonate group of FcDS. Selected bond distances around the Cu^{2+} center are shown in Table 14. Polypyridyl ligand 'tpbn' is spanning between two Cu^{2+} centers. Ferrocene disulphonate is binding to the Cu^{2+} center in a monodentate anti-anti fashion. The central methylene group in the tpbn ligand was found to be disordered in two positions with equal occupancy. The hydrogen bonding interactions are present between free water, acetonitrile and sulphonate oxygens (Figure 27).

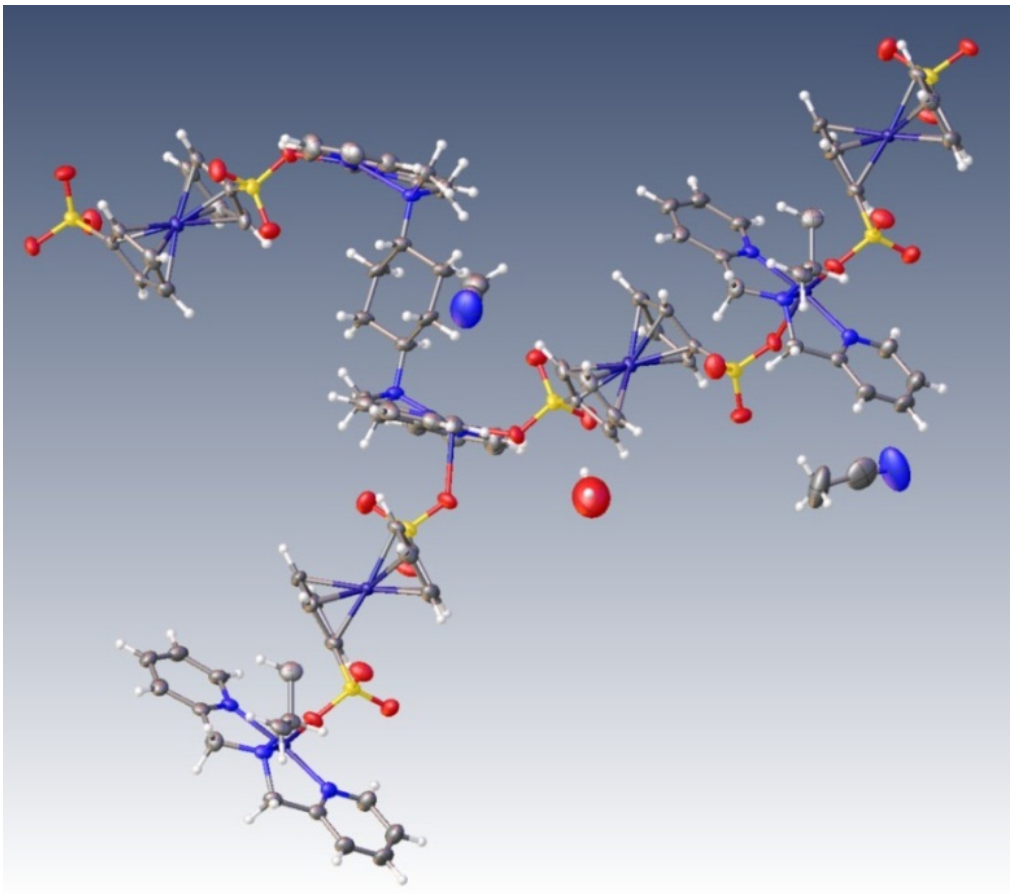

Figure 26. A perspective view of the 2D network in {[Cu_2(tpbn)(FcDS)$_2$]·4CH_3CN·2H_2O}$_n$ (8a).

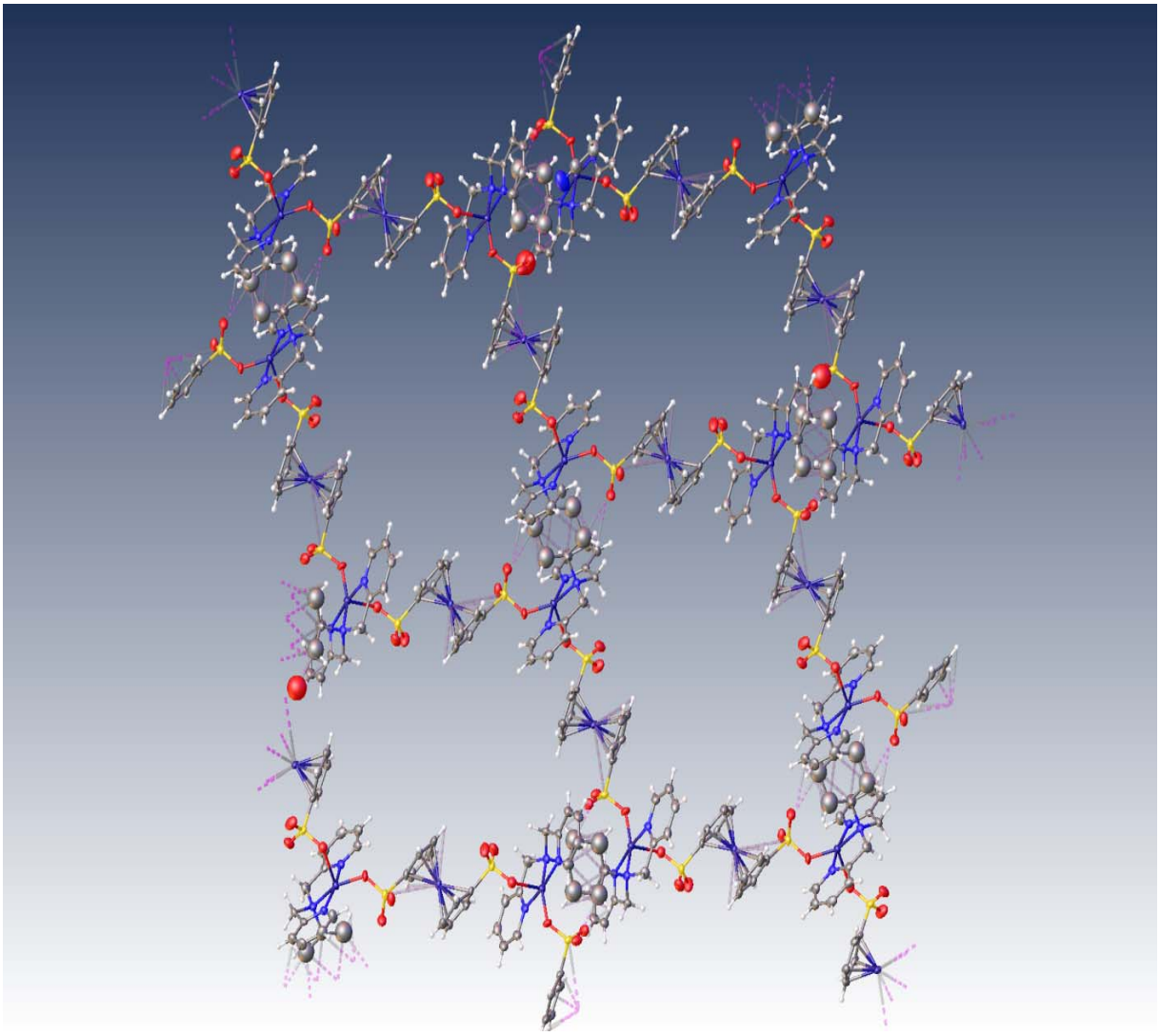

Figure 27. **A perspective view of the pores in 8a**.

Table 13. **Crystal structure data and refinement parameters for 8a**.

Chemical formula	$C_{56}H_{62}S_4Cu_2Fe_2N_{10}O_{14}$
Formula Weight	1466.18
Temperature (K)	170(2)
Wavelength (Å)	0.71073
Crystal system	Monoclinic P
Space group	$P2_1/c$
a (Å)	11.0271(15)
b (Å)	24.390(3)
c (Å)	12.0818(15)
β (°)	113.118(7)
Z	2
Volume ($Å^3$)	2988.5(7)
Density (g/cm^3)	1.629
μ (mm^{-1})	1.392
Theta range	1.67° to 24.21°
F(000)	1508
Reflections Collected	19138
Independent reflections	4786
Reflections with I >2σ(I)	3776
R (int)	0.0397
Number of parameters	408
S (goodness of fit) on F^2	0.944
Final R_1/wR_2 (I >2σ(I))	0.0393/0.1180
Weighted R_1/wR_2 (all data)	0.0560/0.1314
Largest diff. peak and hole ($eÅ^{-3}$)	0.651 and -0.638

Table 14. **Selected bond distances (Å) and bond angles (°) for 8a**.

Bond distances

Cu1-O2	1.988(3)
Cu1-N1	1.983(3)
Cu1-O5$^{\#1}$	2.234(3)
Cu1-N2	2.033(3)
Cu1-N3	1.989(3)

Bond angles

N1-Cu1-N3	165.11(13)	N1-Cu1-O2	95.87(12)
N3-Cu1-O2	98.72(12)	N1-Cu1-N2	82.67(13)
N3-Cu1-N2	82.64(13)	O2-Cu1-N2	159.06(12)
N1-Cu1-O5$^{\#2}$	94.29(11)	N3-Cu1-O5$^{\#2}$	89.79(11)
O2-Cu1-O5$^{\#2}$	85.60(11)	N2-Cu1-O5$^{\#2}$	115.33(11)

Note 1. Numbers in parenthesis are estimated standard deviations.

Note 2. #1 -x+1, -y+1, -z; #2 x-1, -y+3/2, z-1/2

Powder X-ray Studies

Powder X-ray diffraction was used to analyze Na_2FcDC, $(NH_4)_2FcDS$ and all compounds to check their crystallinity and similarity. Figures 28-36 show the PXRD patterns obtained. It was found during the analysis that all the samples except the Fe^{3+} complexes were crystalline. On comparison of the powder patterns of the compounds with that of the linkers, it was found that linker is present in all the compounds. **7** and **8** have fewer peaks compared to other compounds which point towards higher symmetry in these complexes. Broad peaks also indicate the presence of water molecules. Indexing was found to be difficult due to the large molecular formula for these complexes.

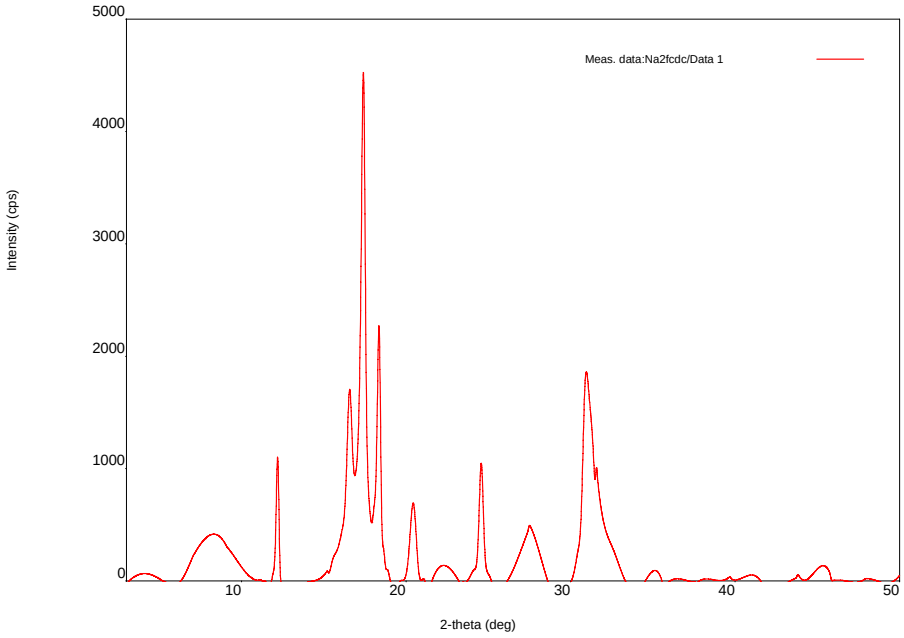

Figure 28. **PXRD pattern for Na_2FcDC**.

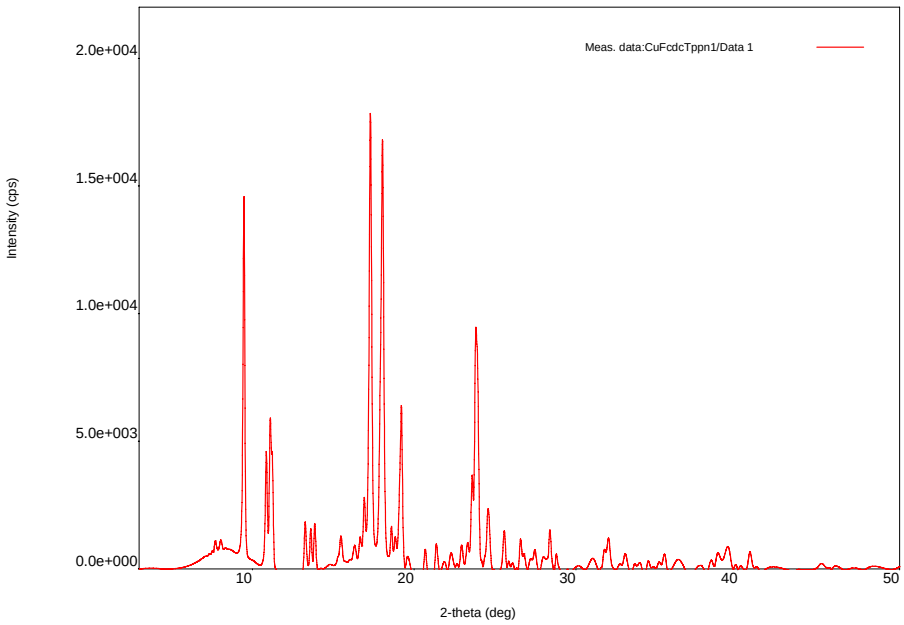

Figure 29. **PXRD pattern for 1**.

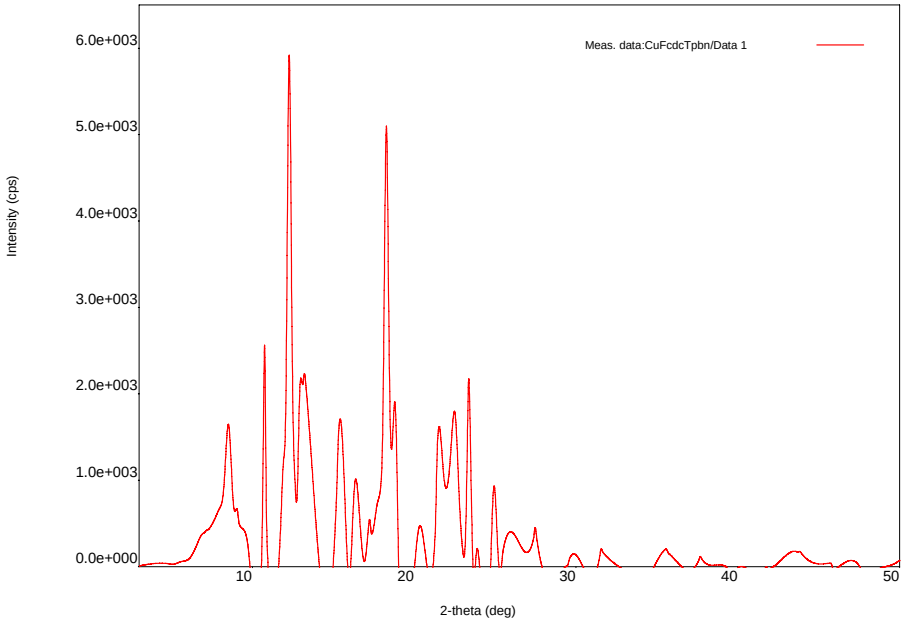

Figure 30. **PXRD pattern for 2**.

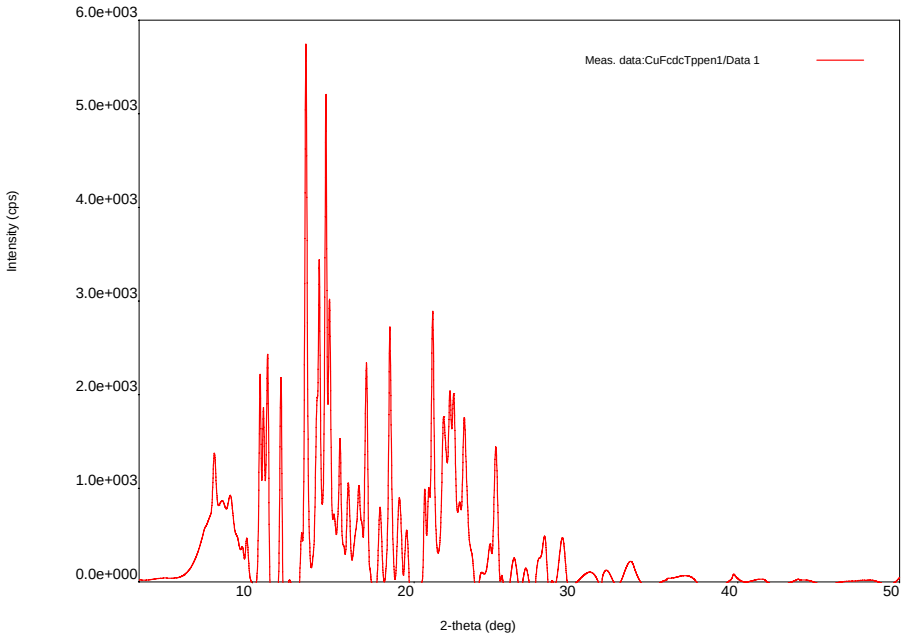

Figure 31. PXRD pattern for 3.

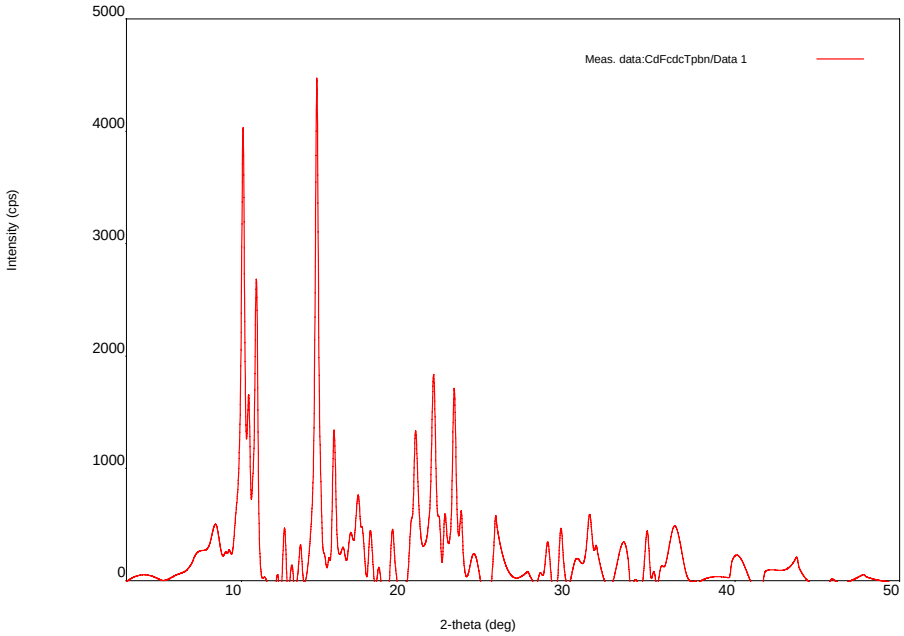

Figure 32. PXRD pattern for 4.

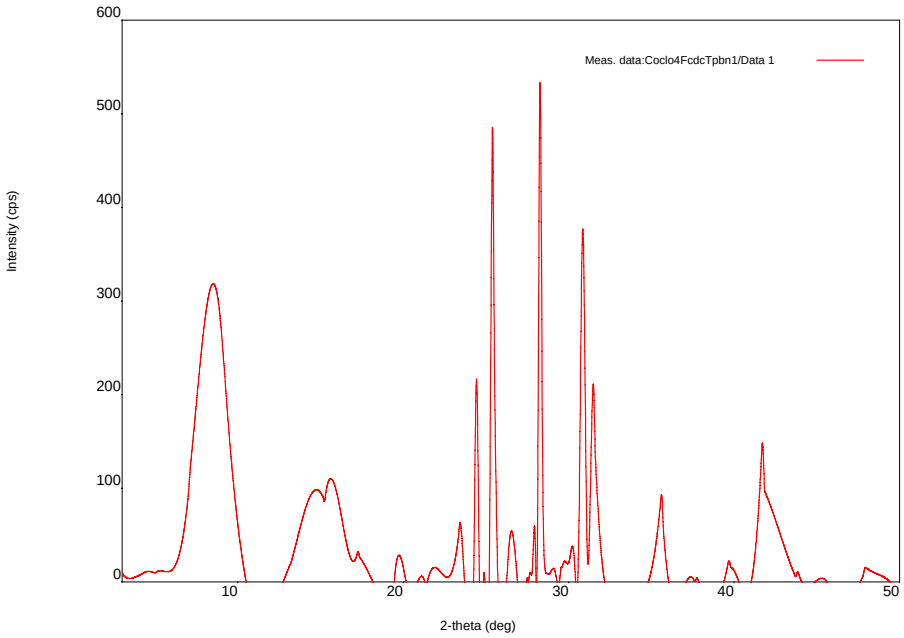

Figure 33. **PXRD pattern for 6**.

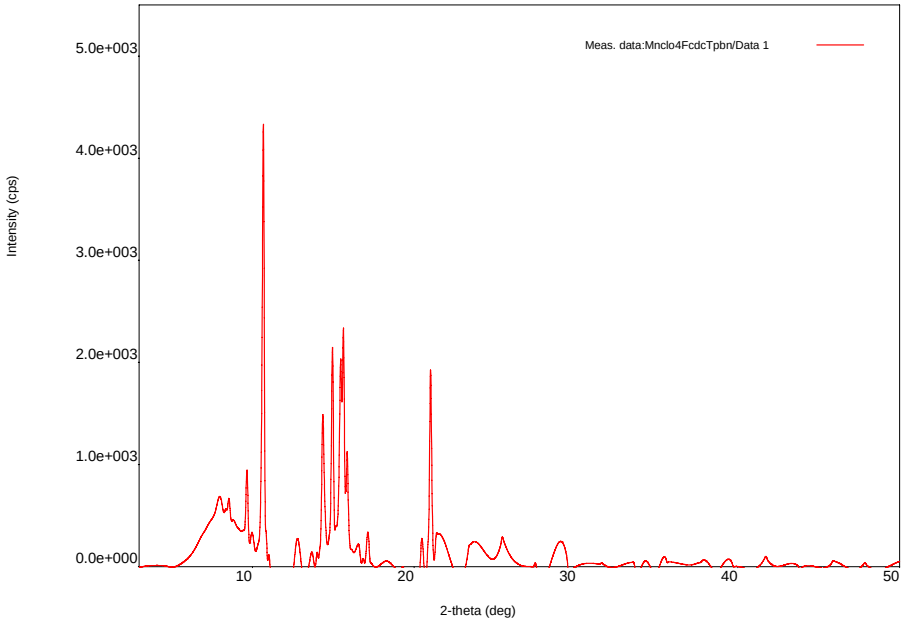

Figure 34. **PXRD pattern for 7**.

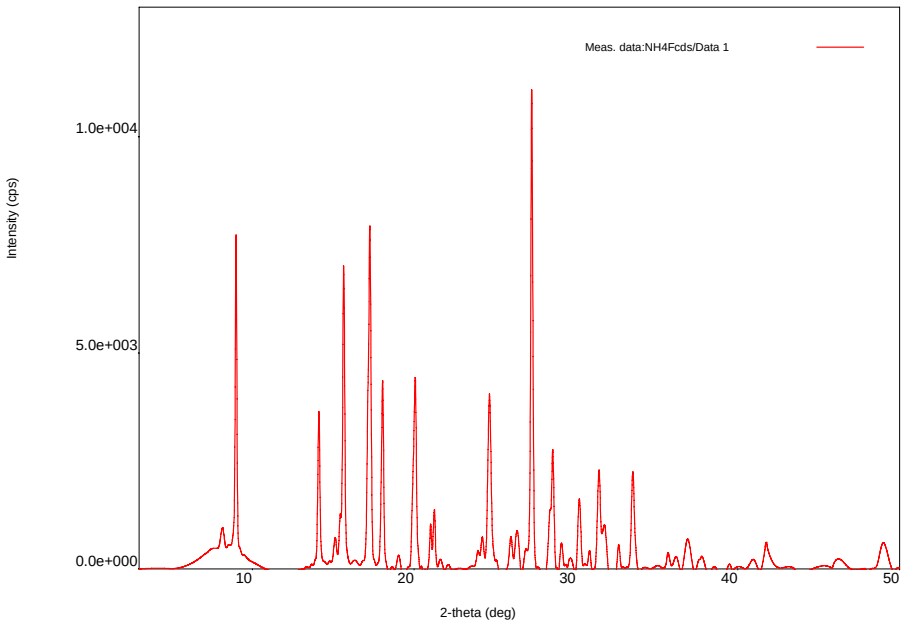

Figure 35. PXRD pattern for $(NH_4)_2$FcDS.

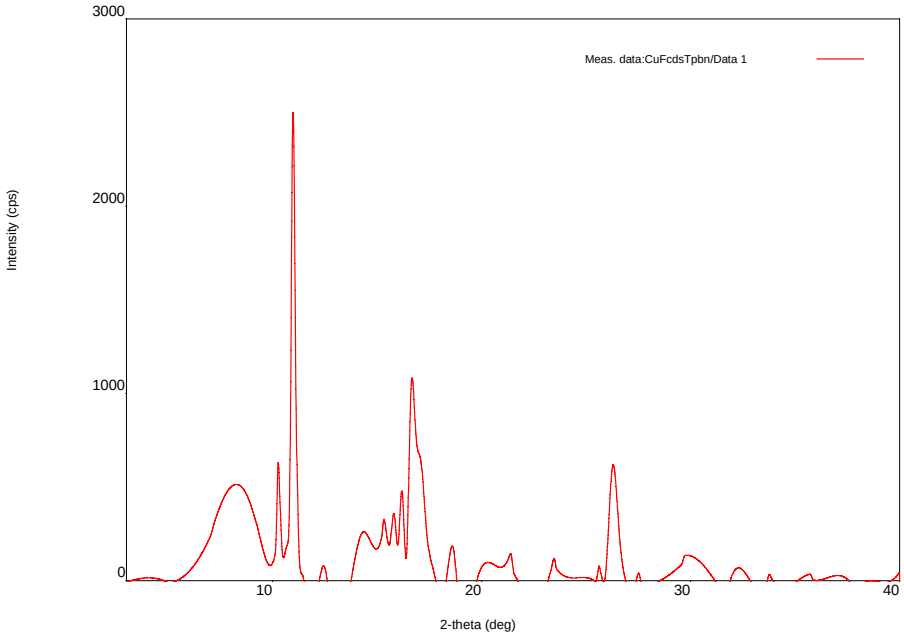

Figure 36. PXRD pattern for 8.

Thermal Gravimetric Analysis

In order to study their thermal stabilities, these compounds were examined by thermal gravimetric analysis between 25-500 ºC. In TGA spectra of all compounds with FcDC, a spike at around 200 ºC was observed which might be due to the release of CO_2 gas. As is evident from the data, most of the compounds are stable up to 200 ºC.

Table 15. **Thermal gravimetric analysis of the compounds**.

S. No.	Compound	Step I % Loss calc. (found) [molecules lost]	Step II % Loss calc. (found) [molecules lost]
1.	$[Cu_4(tppn)_2(FcDC)_2(H_2O)_4](ClO_4)_4 \cdot 2H_2O$	53.18 (54.04) [$6H_2O$ + 2FcDC + C_6NH_6 + $4ClO_4^-$]	46.77 (46.27) [2tppn + 4 Cu - C_6NH_6]
2.	$[Cu_4(tpbn)_2(FcDC)_2(H_2O)_4](ClO_4)_4 \cdot 6H_2O$	6.31 (6.37) [$8H_2O$]	82.55 (83.61) [$2H_2O$ + 2FcDC + 2tpbn + $4ClO_4^-$]
3.	$[Cu_4(tppen)_2(FcDC)_2(H_2O)_4](ClO_4)_4 \cdot 6H_2O$	1.56 (1.95) [$2H_2O$]	25.03 (24.86) [$8H_2O$ + $4ClO_4^-$]
4.	$[Cd_4(tpbn)_2(FcDC)_2(H_2O)_4](ClO_4)_4$	7.23 (7.67) [$4H_2O$ + ClO_4^-]	39.48 (40.91) [C_6NH_6 + 2FcDC + $3ClO_4^-$]
5.	$\{[Fe_2(\mu\text{-}O)(tpbn)(FcDC)](ClO_4)_2 \cdot 2H_2O\}_n$	3.31 (2.80) [$2H_2O$]	84.93 (84.48) [FcDC + tpbn + $2ClO_4^-$]
6.	$[Co_4(tpbn)_2(FcDC)_2(H_2O)_4](ClO_4)_4 \cdot 4H_2O \cdot 1.5KClO_4$	5.91 (6.81) [$8H_2O$]	84.39 (86.29) [2FcDC + 2tpbn + $1.5KClO_4$ + $4ClO_4^-$]
7.	$[Mn_4(tpbn)_2(FcDC)_2(H_2O)_4](ClO_4)_4 \cdot KClO_4$	1.97 (1.93) [$2.5H_2O$]	16.00 (15.37) [$1.5H_2O$ + $KClO_4$ + $2ClO_4^-$]
8.	$[Cu_2(tpbn)(FcDS)_2]_n \cdot n\{[Cu_2(tpbn)(H_2O)_2](ClO_4)_4\}$	8.13 (8.04) [$2H_2O$ + 1. $5ClO_4^-$]	41.08 (40.19) [2FcDS + $2.5ClO_4^-$]
9.	$\{[Fe_2(\mu\text{-}O)(tpbn)(FcDS)](ClO_4)_2 \cdot 4H_2O\}_n$	6.03 (6.36) [$4H_2O$]	12.48 (11.49) [$1.5ClO_4^-$]

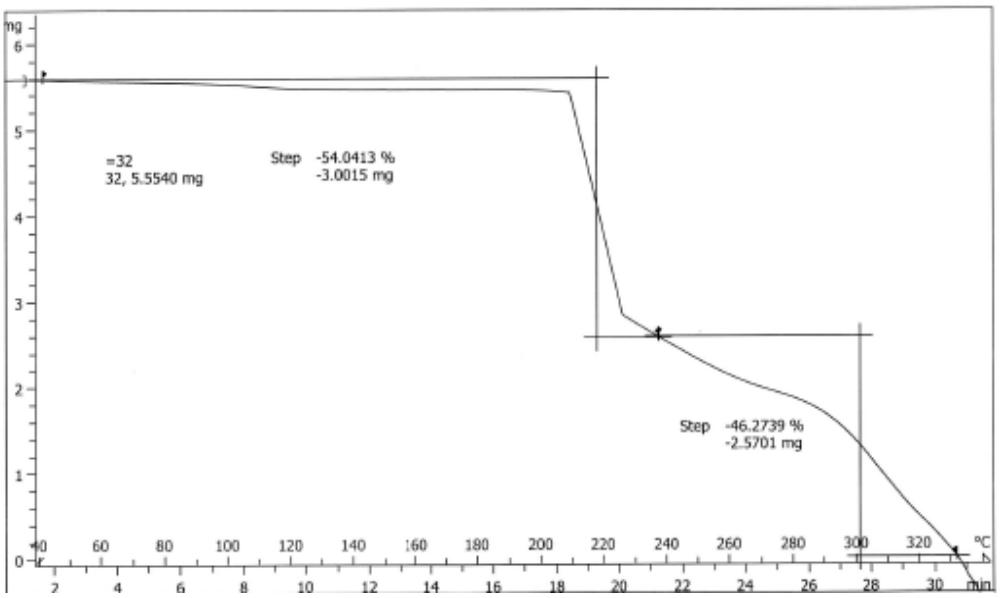

Figure 37. **TGA of 1**.

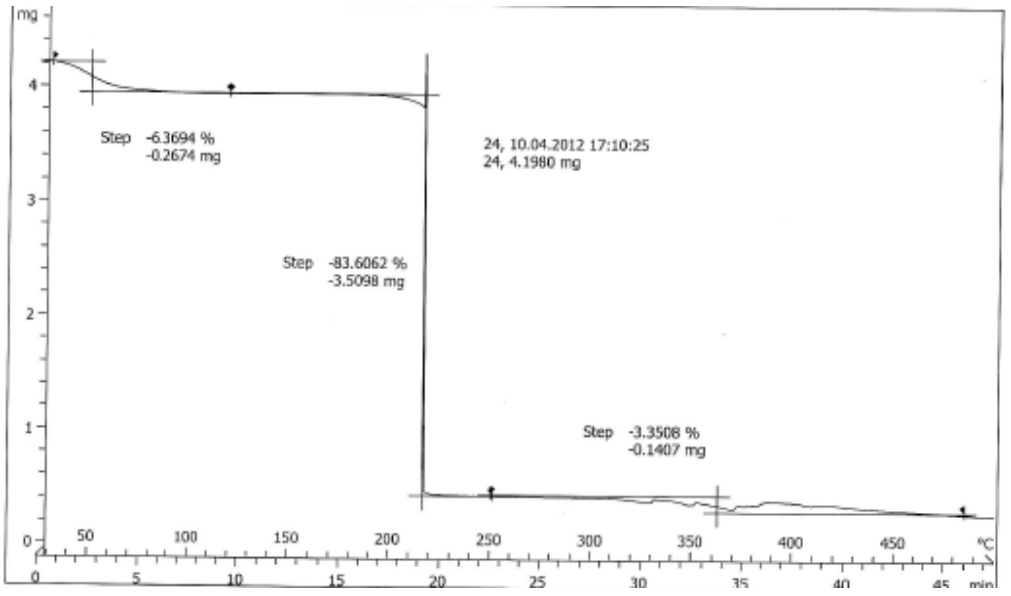

Figure 38. **TGA of 2**.

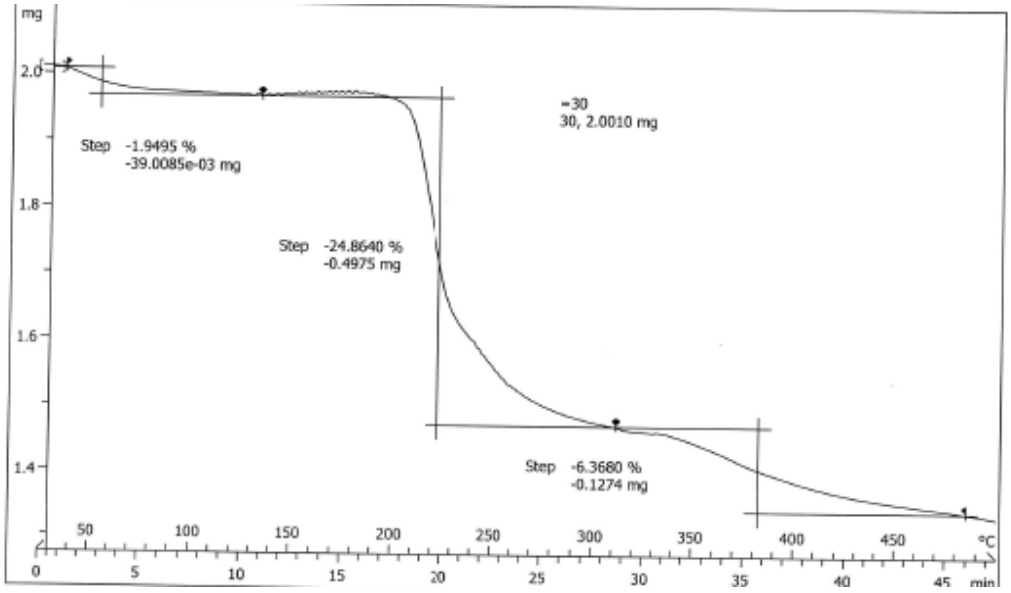

Figure 39. **TGA of 3**.

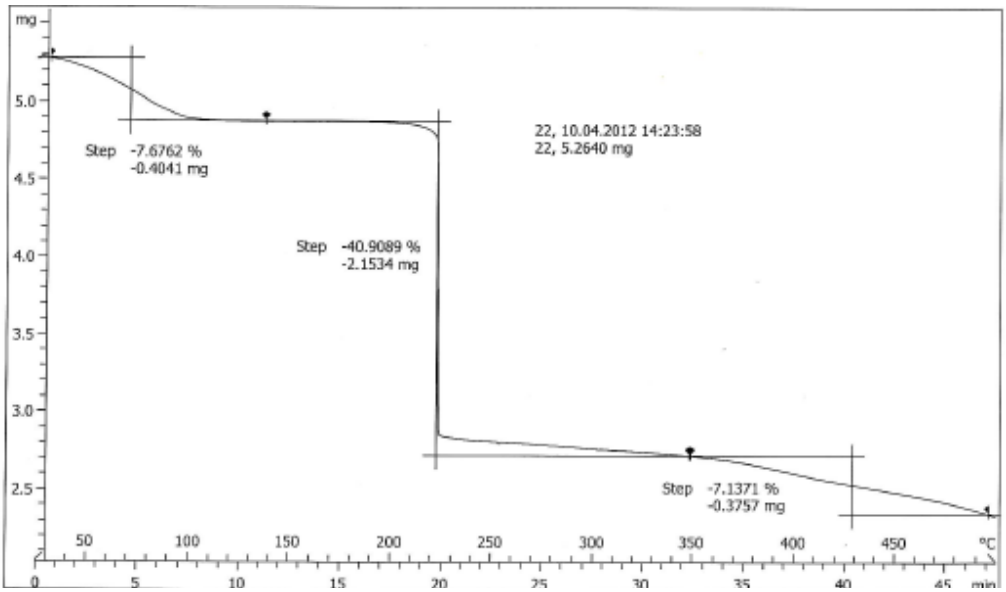

Figure 40. **TGA of 4**.

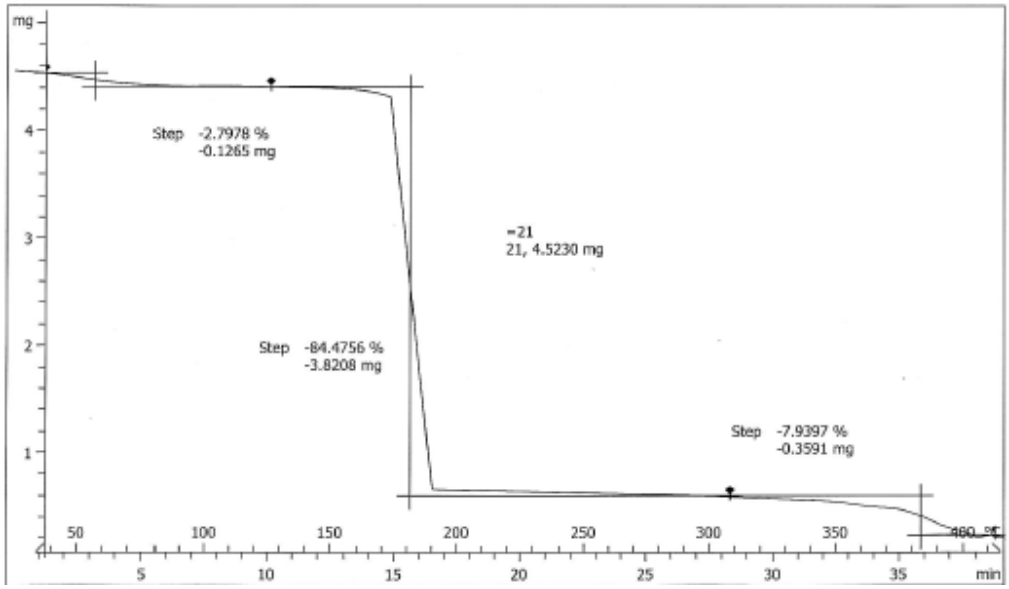

Figure 41. **TGA of 5**.

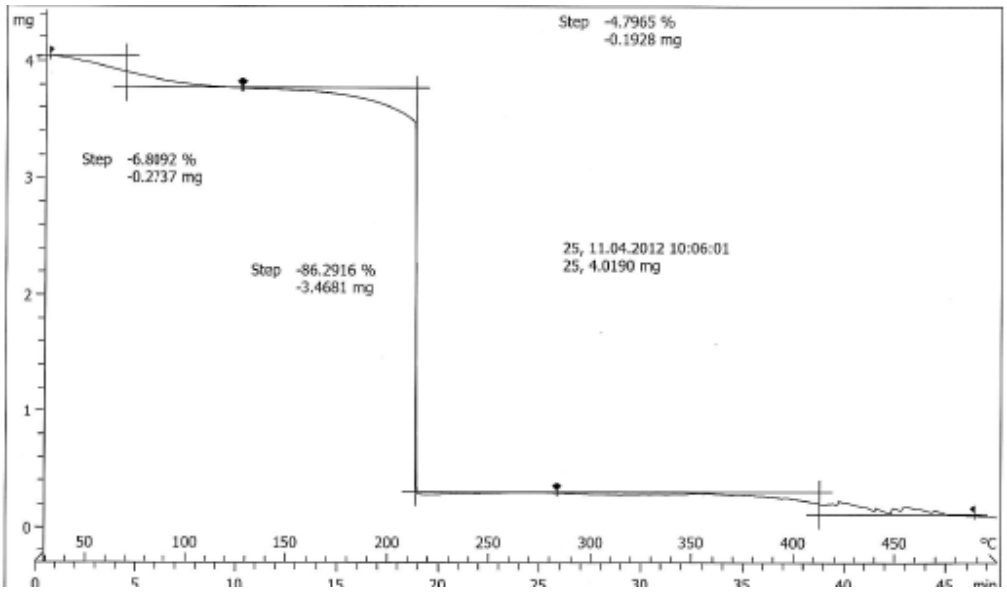

Figure 42. **TGA of 6**.

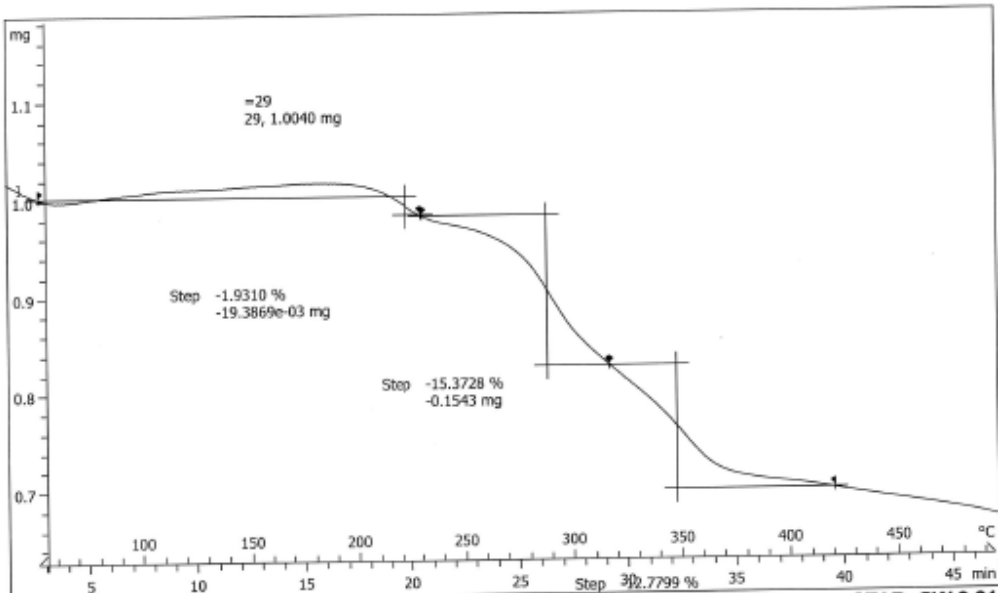

Figure 43. **TGA of 7**.

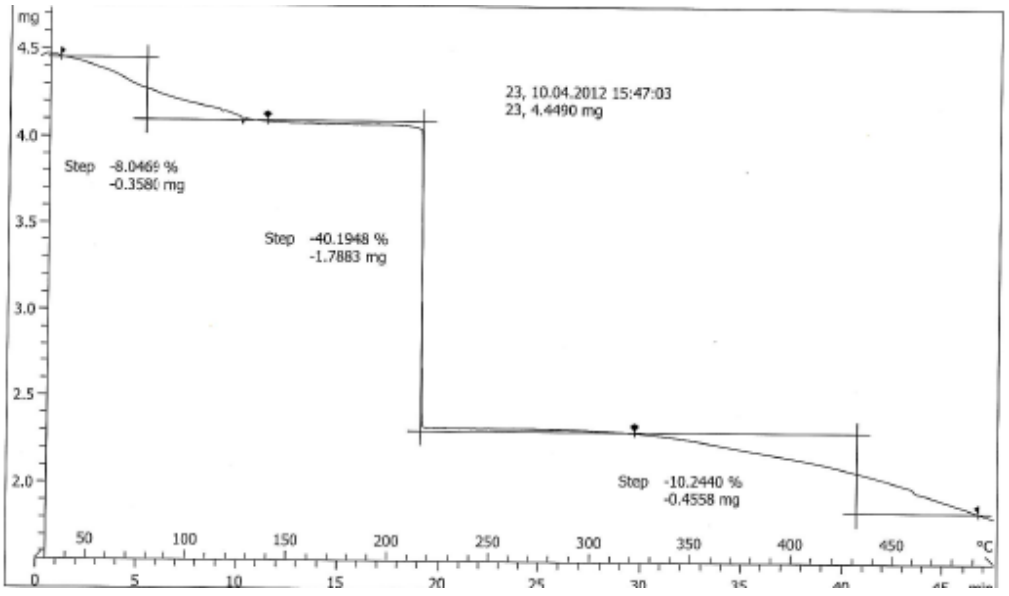

Figure 44. **TGA of 8**.

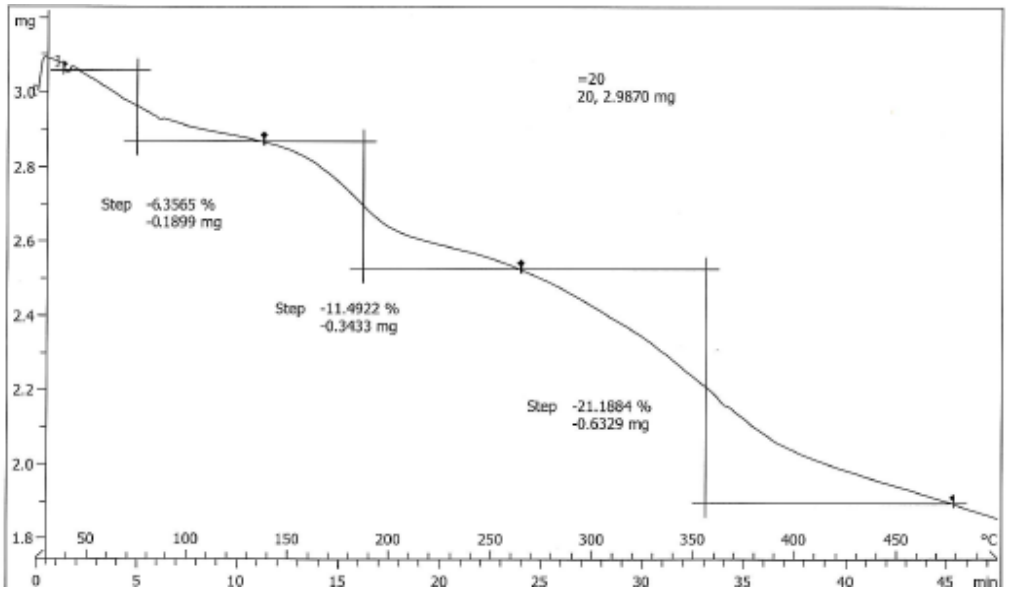

Figure 45. **TGA of 9**.

Differential Scanning Calorimetry

The metal complexes were studied by differential scanning calorimetry between 25-300 ºC at a scan rate of 10º per minute to understand the thermodynamics of the interactions involved. In addition, DSC results were correlated to the TGA results to confirm the thermal behavior of the systems and it was found that indeed, most of the complexes are stable up to 200 ºC with an exothermic change occurring at that temperature which can be attributed to the release of CO_2 in case of compounds with FcDC as a linker and SO_3 in case of compounds with FcDS as a linker. Selected DSC scans are shown below (Figures 46-50).

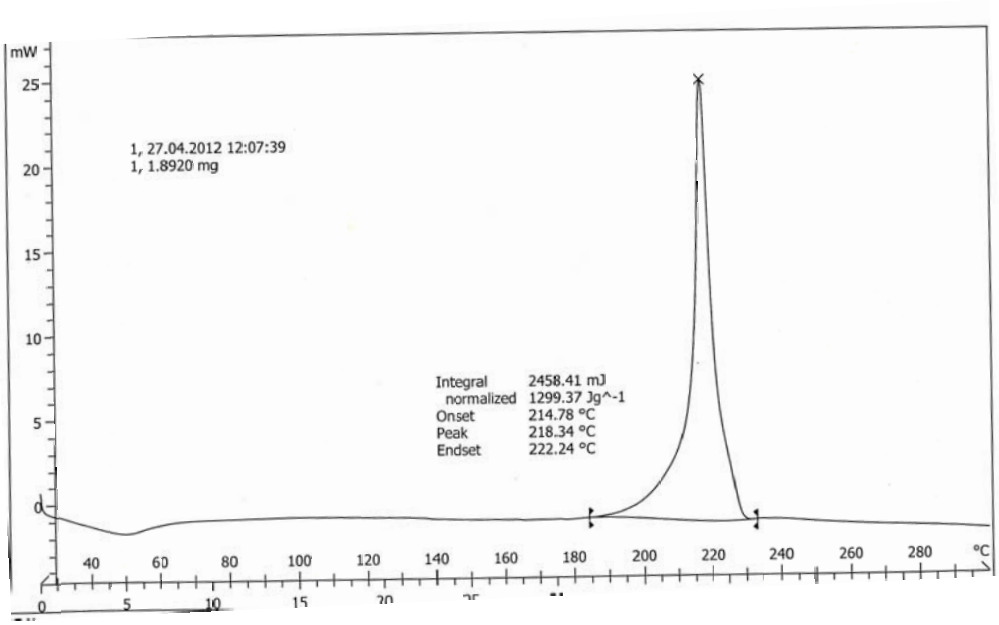

Figure 46. **DSC of 2**.

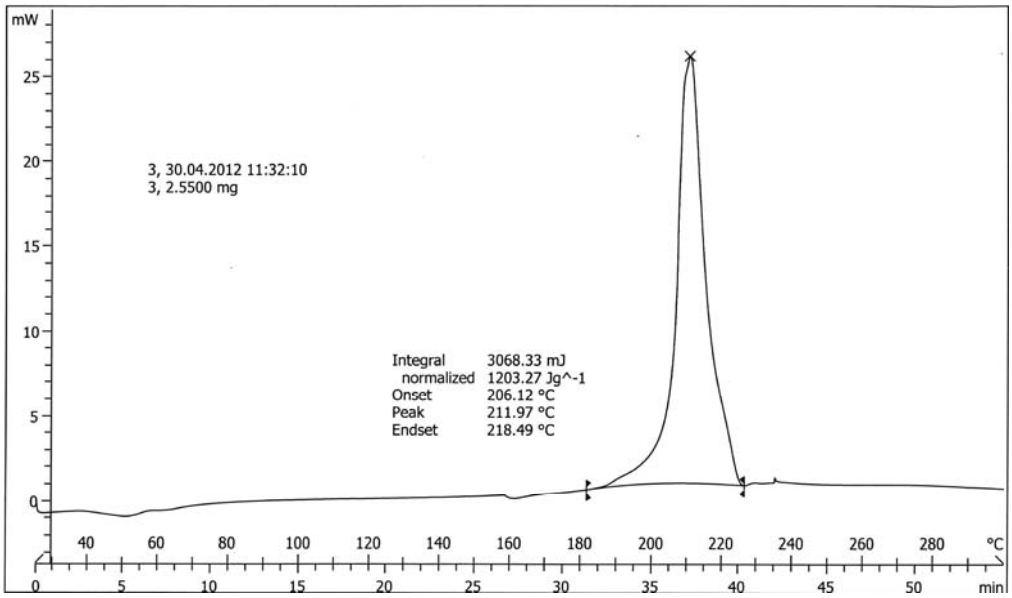

Figure 47. **DSC of 3**.

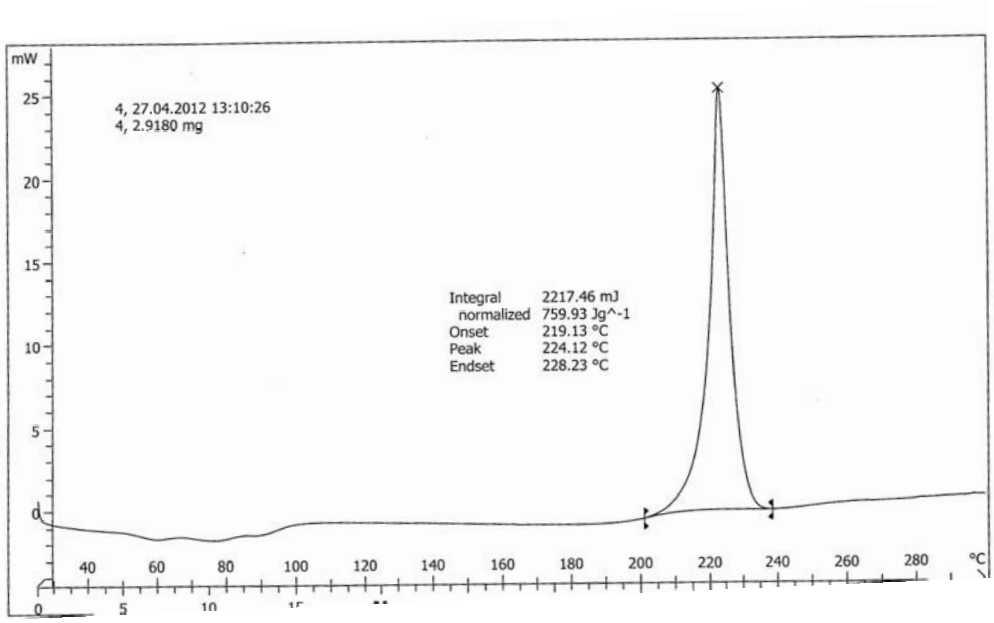

Figure 48. **DSC of 4**.

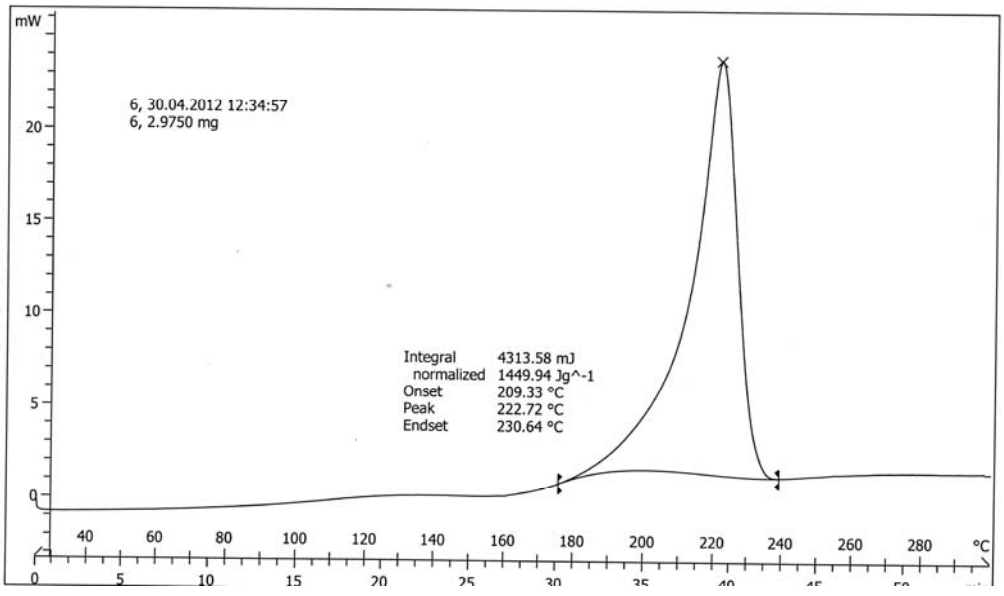

Figure 49. **DSC of 6**.

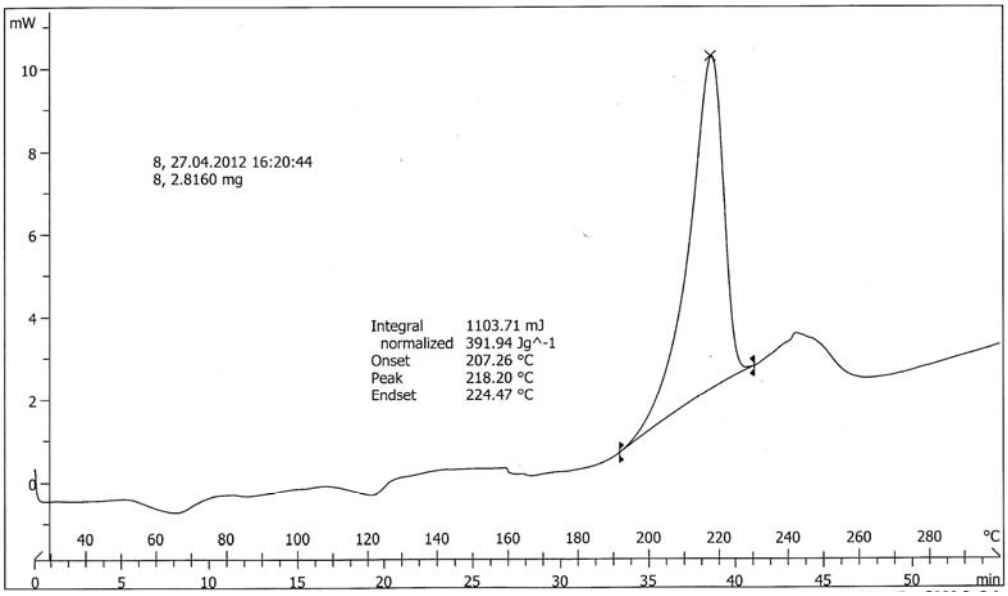

Figure 50. **DSC of 8**.

Proposed Structures

Based on elemental analysis and mass spectrometry data, the proposed structures of the compounds are shown in Figure 46. Complexes of Cu^{2+}(1, 2, 3), Cd^{2+}, Co^{2+} and Mn^{2+} have a rectangular geometry while the one with Fe^{3+} ion is a 2D coordination polymer. In (a) the metal center is shown to have five bonds which is correct for Cu^{2+} as it prefers to have pentacoordination, while the other metal ions (Cd^{2+}, $Co^{2+}$and Mn^{2+}) prefer to have hexacoordination. Ligand tpbn is spanning between the two metal centers thus satisfying three coordination sites on each metal center. Carboxylate anion is binding in a monodentate fashion thus occupying the fourth site while the fifth site is occupied by a solvent molecule, e.g., water. For other metal centers, which prefer to have hexacoordination, two solvent molecules bind to the metal center. In case of Fe^{3+}, the Fe_2(μ-O)(μ-biscarboxylato) unit is spanning in one direction while the tpbn unit is spanning between the two parallel Fe_2(μ-O)(μ-biscarboxylato) units in the other, thus making it a 2D coordination polymer.

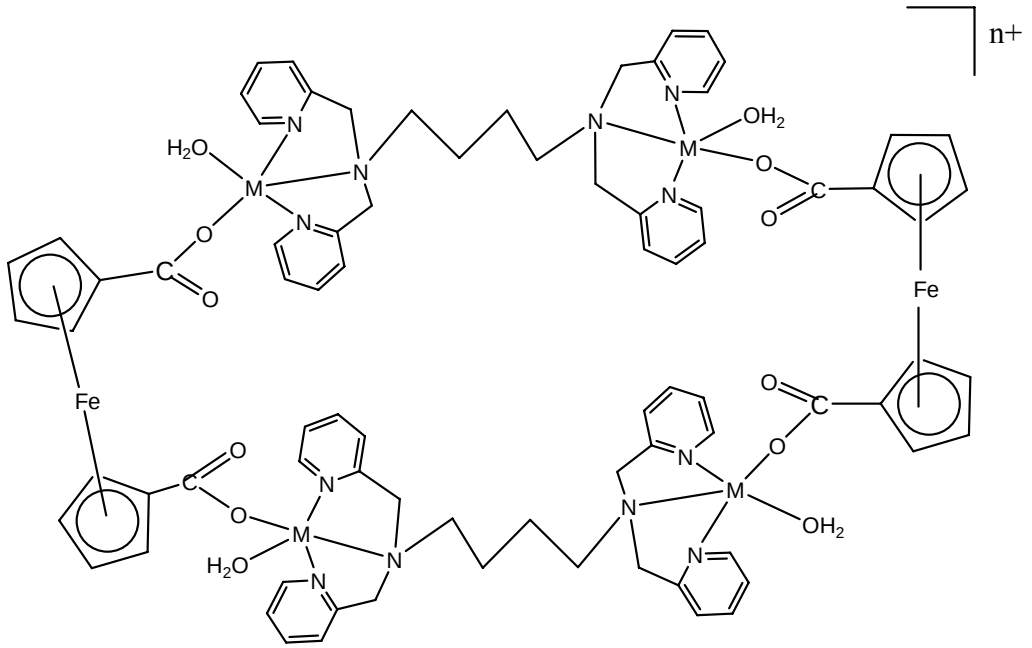

(a)

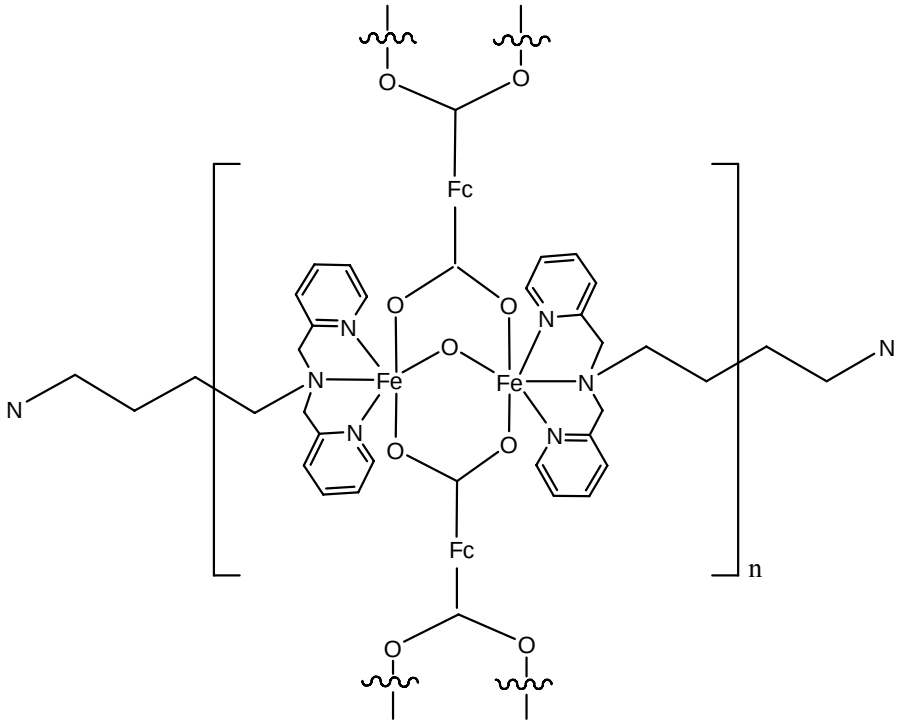

(b)

Figure 46. (a) Proposed Structure for Compounds with Cu^{2+}, Cd^{2+}, Mn^{2+}, Co^{2+} ions. (b) Proposed Structure for the Compound with Fe^{3+} ion.

Chapter IV

Conclusions

Ferrocene dicarboxylate and ferrocene disulphonate have rarely been employed to synthesize MOFs despite their exceptional properties. This work utilized FcDC and FcDS as linkers and polypyridyl moieties as ancillary ligands. In case of FcDC, discrete rectangular MOFs based on Cu^{2+}, Cd^{2+}, Co^{2+} and Mn^{2+} were obtained while a 2D coordination polymer was obtained with Fe^{3+}. Use of FcDS resulted in 2D MOF for Cu^{2+} (confirmed by single crystal X-ray diffractometry) and 1D coordination polymer for Fe^{3+}. Thermal gravimetric analysis and differential scanning calorimetry showed that most of these compounds are stable up to 200 ºC. Since all compounds are composed of ferrocene, their electro-chemical behavior can be studied. Further, these compounds can be studied for their use as sensors, gas storage materials, catalysts and for host-guest chemistry.

References

1. (a) Xu, R.; Pang, W.; Yu, J.; Huo, Q.; Chen, J. *Chemistry of Zeolites & Related Porous Materials: Synthesis & Structure*; Wiley-Interscience, 2007. (b) Bruce, D. W.; O'Hare, D.; Walton, R. I. *Porous Materials (Inorganic Materials Series)*; Wiley, 2010.
2. Kitagawa, S.; Kitaura, R.; Noro, S. *Angew. Chem. Int. Ed*. **2004**, *43*, 2334.
3. Hoskins, B. F.; Robson, R. *J. Am. Chem. Soc*. **1990**, *112*, 1546.
4. Eddaoudi, M.; Moler, D. B.; Li, H.; Reineke, T. M.; O'Keeffe, M.; Yaghi, O. M. *Acc. Chem. Res.* **2001**, *34*, 319.
5. Tranchemontagne, D. J.; Mendoza-Corte´s, J. L.; O'Keeffe, M.; Yaghi, O. M. *Chem. Soc. Rev.* **2009**, *38*, 1257.
6. Christoph, J. *Dalton Trans.* **2003**, 2781.
7. Courtesy: Ms. Sadhika Khullar, PhD scholar, IISER Mohali.
8. Leznoff, D. B.; Xue, B.; Patrick, B. O.; Sanchez, V.; Thompson, R. C. *Chem. Commun*. **2001**, 259.
9. Stock, N.; Biswas, S. *Chem. Rev.* **2012**, Special Issue – Metal Organic Frameworks.
10. Mingos, D. M. P.; Baghurst, D. R. *Chem. Soc. Rev*. **1991**, *20*, 1.
11. Fernandez-Bertran, J. F. *Pure Appl. Chem*. **1999**, *71*, 581.
12. Rabenau, A. *Angew. Chem. Int. Ed*. **1985**, *24*, 1026.
13. Ni, Z.; Masel, R. I. *J. Am. Chem. Soc.* **2006**, *128*, 12394.
14. Meek, S. T.; Greathouse, J. A.; Allendorf, M. D. *Adv. Mater*. **2011**, *23*, 249.
15. Pichon, A.; Lazuen-Garay, A.; James, S. L. *CrystEngComm.* **2006**, *8*, 211.
16. Pichon, A.; James, S. L. *CrystEngComm.* **2008**, *10*, 1839.
17. Friscic, T.; Fabian, L. *CrystEngComm.* **2009**, *11*, 743.
18. Li, J.; Kuppler, R.; Zhou, H. *Chem. Soc. Rev*. **2009**, *38*, 1477.
19. Kondo, M.; Yoshitomi, T.; Seki, K.; Matsuzaka, H.; Kitagawa, S. *Angew. Chem. Int. Ed.* **1997**, *36*, 1725.

20. Han, S. S.; Mendoza-Corte´ s, J. L.; Goddard, W. A. *Chem. Soc. Rev*. **2009**, *38*, 1460.
21. Murray, L. J.; Dinca, M.; Long, J. R. *Chem. Soc. Rev.* **2009**, *38*, 1294.
22. Dybtsev, D.; Chun, H.; Yoon, S. H.; Kim, D.; Kim, K. *J. Am. Chem. Soc*. **2004**, *126*, 32.
23. Schlichte, K.; Kratzke, T.; Kaskel, S. *Microporous and Mesoporous Materials*. **2004**, *73,* 81.
24. Achmann, A.; Hagen, G.; Kita, J.; Malkowsky, I. M.; Kiener, C.; Moos, R. *Sensors.* **2009**, *9*, 1574.
25. Horike, S.; Dinca, M.; Tamaki, K.; Long, J. R. *J. Am. Chem. Soc.* **2008**, *130*, 5854.
26. Gándara, F.; Gomez-Lor, B.; Gutiérrez-Puebla, E.; Iglesias, M.; Monge, M. A.; Proserpio, D. M.; Snejko, N. *Chem. Mater.* **2008**, *20,* 72.
27. Horcajada, P.; Serre, C.; Vallet-Regí, M.; Sebban, M.; Taulelle, F.; Férey, G. *Angew. Chem. Int. Ed*. **2006**, *45*, 5974.
28. McKinlay, A. C.; Xiao, B.; Wragg, B. S.; Wheatley, P. S.; Megson, I. L.; Morris, R. *J. Am. Chem. Soc.* **2008**, *130*, 10440.
29. Kealy, T. J.; Pauson, P. L. *Nature*. **1951**, *168*, 1039.
30. Wilkinson, G.; Rosenblum. M.; Whiting, M. C.; Woodward, R. B. *J. Am. Chem. Soc.* **1952**, *74*, 2125.
31. Woodward, R. B.; Rosenblum, M.; Whiting, M. C. *J. Am. Chem. Soc.* **1952**, *74*, 3458.
32. Jutzi, P.; Lenze, N.; Neumann, B.; Stammler, H. G. *Angew. Chem. Int. Ed.* **2001**, *40*, 1424.
33. Kuhnert, J.; Ruffer, T.; Ecorchard, P.; Brauer, B.; Lan, Y.; Powell, A. K., Lang, H. *Dalton Trans*. **2009**, 4499.
34. Das, N.; Arif, A. M.; Stang, P. J. *Inorg. Chem*. **2005**, *44*, 5798.
35. Mereacre, V.; Prodius, D.; Ako, A. M.; Shova, S.; Turta, C.; wurst, K.; Jaitner, P.; Powell, A. K. *Polyhedron*. **2009**, *28*, 3551.
36. Rausch, M. D.; Ciappenelli, D. J.; *J. Organomet. Chem.* **1967**, *10*, 127.
37. Weinmayr, V. *J. Am. Chem. Soc.* **I955**, *77*, 3009.
38. Yang, L.; Bian, F.; Yan, S.; Liao, D.; Cheng, P.; Jiang, Z. *Inorg. Chem. Commun*. **2003**, *6*, 1188.

39. Meng, X.; Hou, H.; Li, G.; Ye, B.; Ge, T.; Fan, Y.; Zhu, Y.; Sakiyama, H. *J. Organomet. Chem.* **2004**, *689*, 1218.
40. Cote, A. P.; Shimizu, G. K. H. *Coord. Chem. Rev.* **2003**, *245*, 49.
41. Personal communication with Ms. Sadhika Khullar, PhD scholar, IISER Mohali.

Appendix

Mass spectra of the Compounds

Mass spectrum for $[Cu_2(tpbn)(FcDS)_2]_n \cdot n\{[Cu_2(tpbn)(H_2O)_2](ClO_4)_4\}$

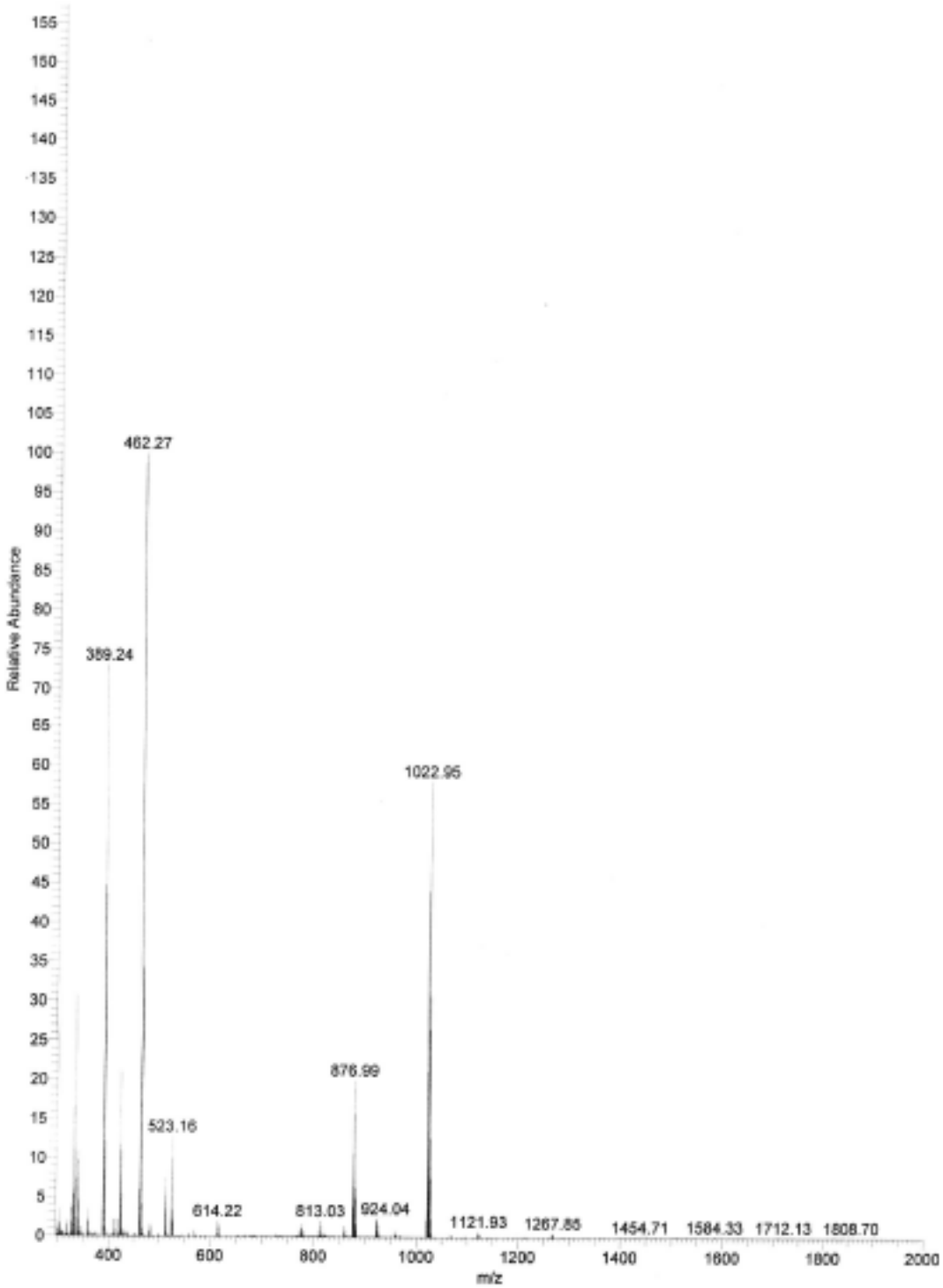

Mass spectrum for $\{[Fe_2(\mu\text{-}O)(tpbn)(FcDS)](ClO_4)_2 \cdot 4H_2O\}_n$

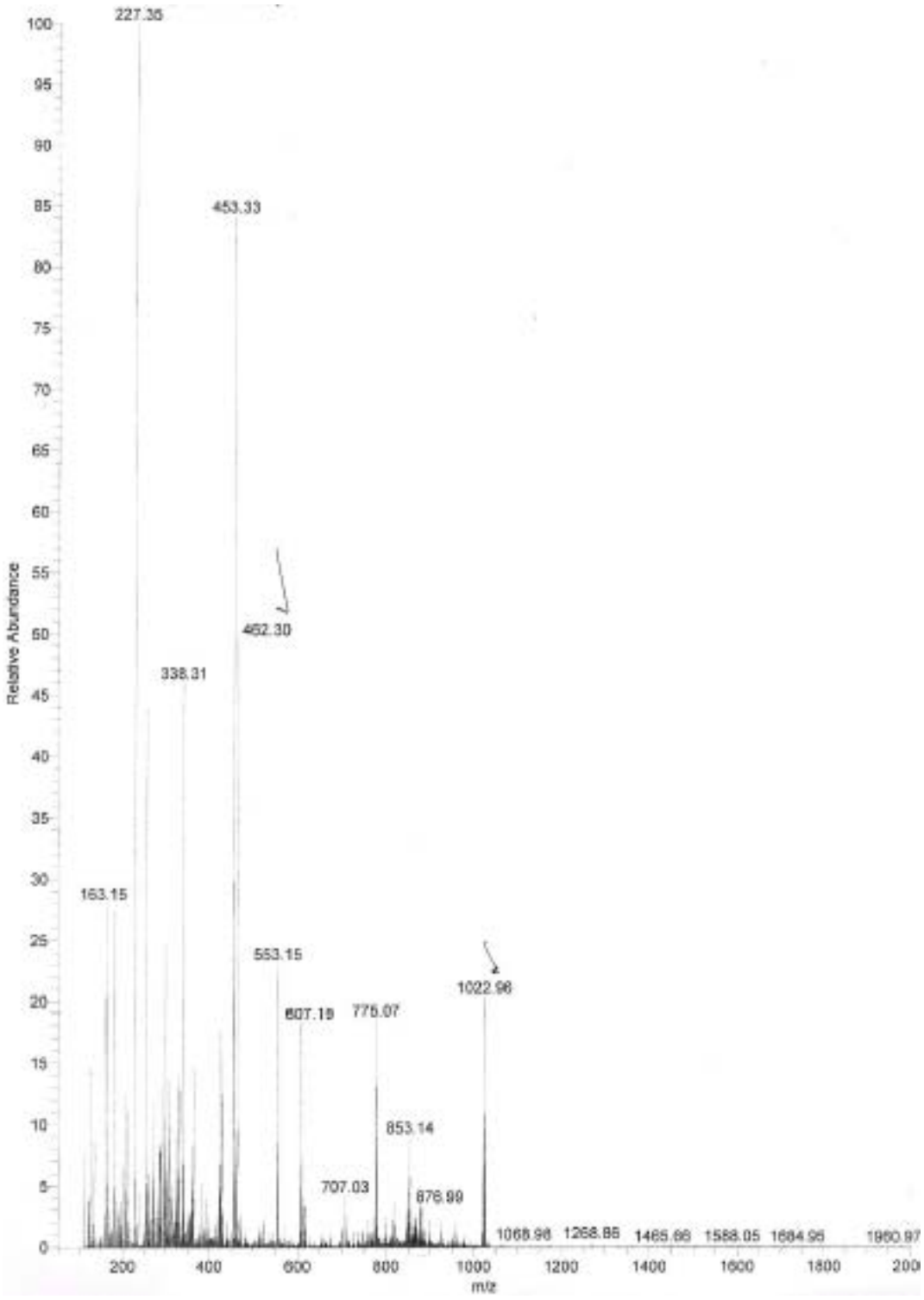

Mass spectrum for $[Cu_4(tpbn)_2(FcDC)_2(H_2O)_4](ClO_4)_4 \cdot 6H_2O$

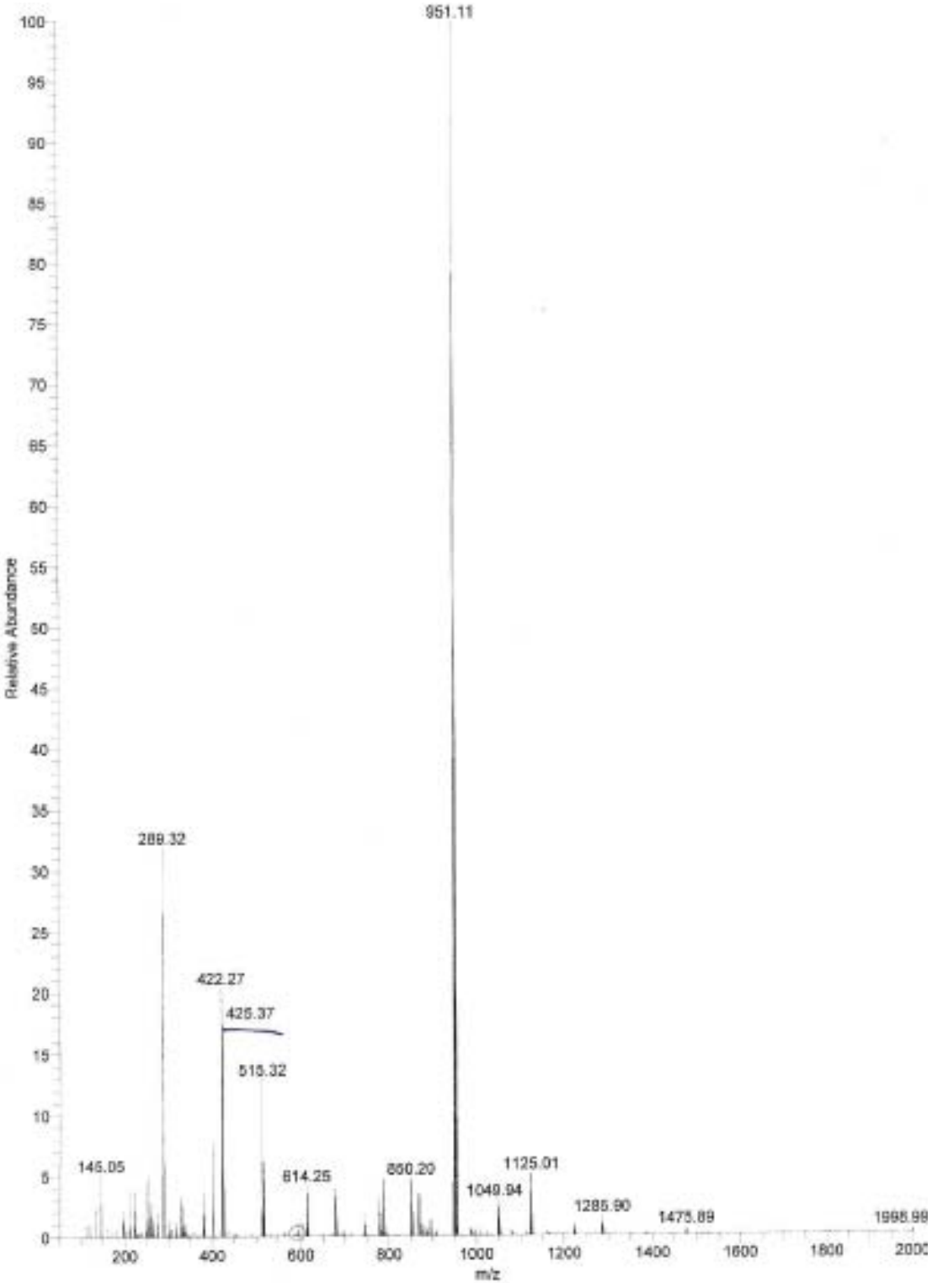

Mass spectrum for $[Co_4(tpbn)_2(FcDC)_2(H_2O)_4](NO_3)_4 \cdot 4H_2O \cdot 1.5KClO_4$

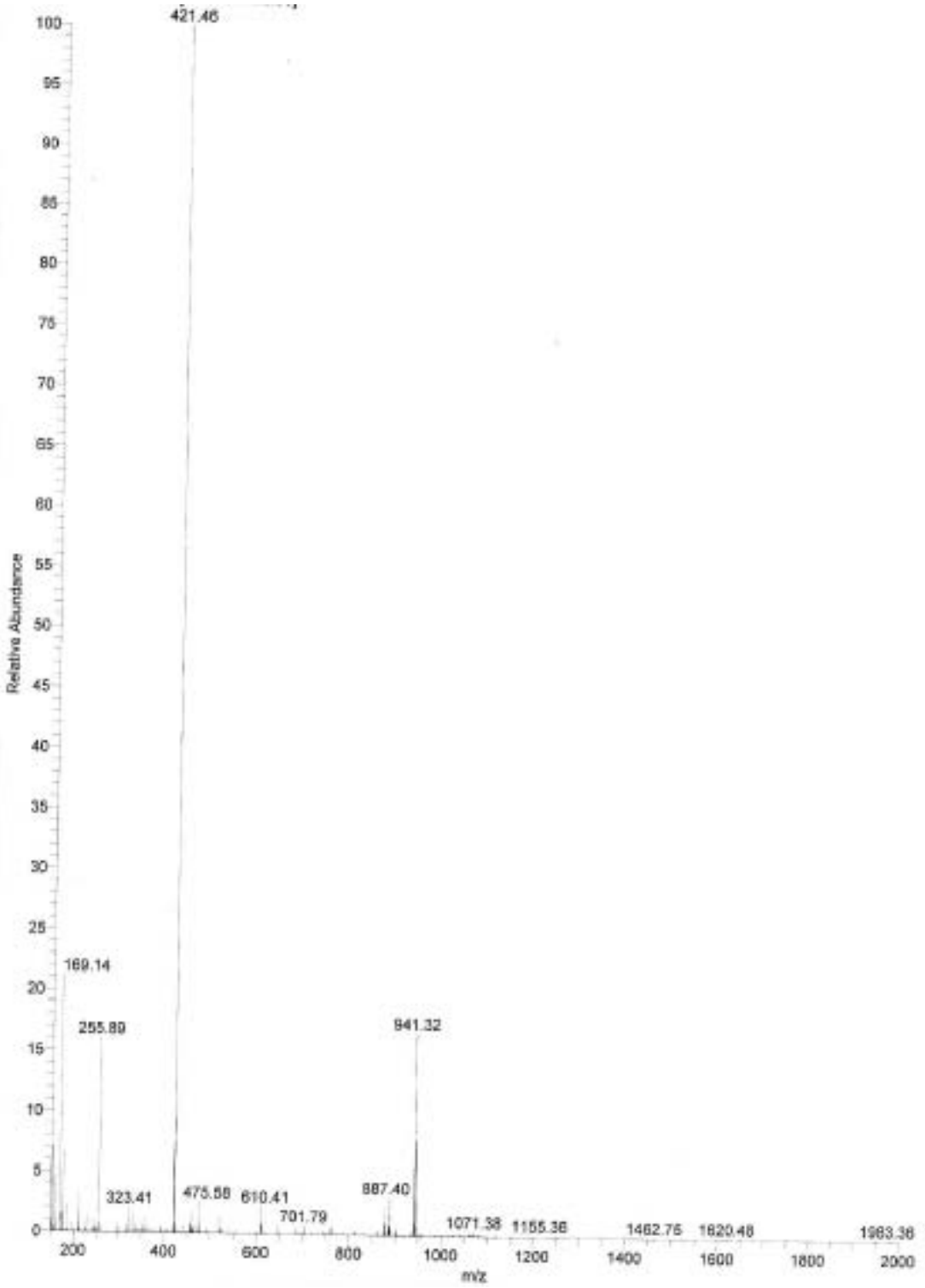

Mass spectrum for $\{[Fe_2(\mu\text{-}O)(tpbn)(FcDC)](ClO_4)_2 \cdot 2H_2O\}_n$

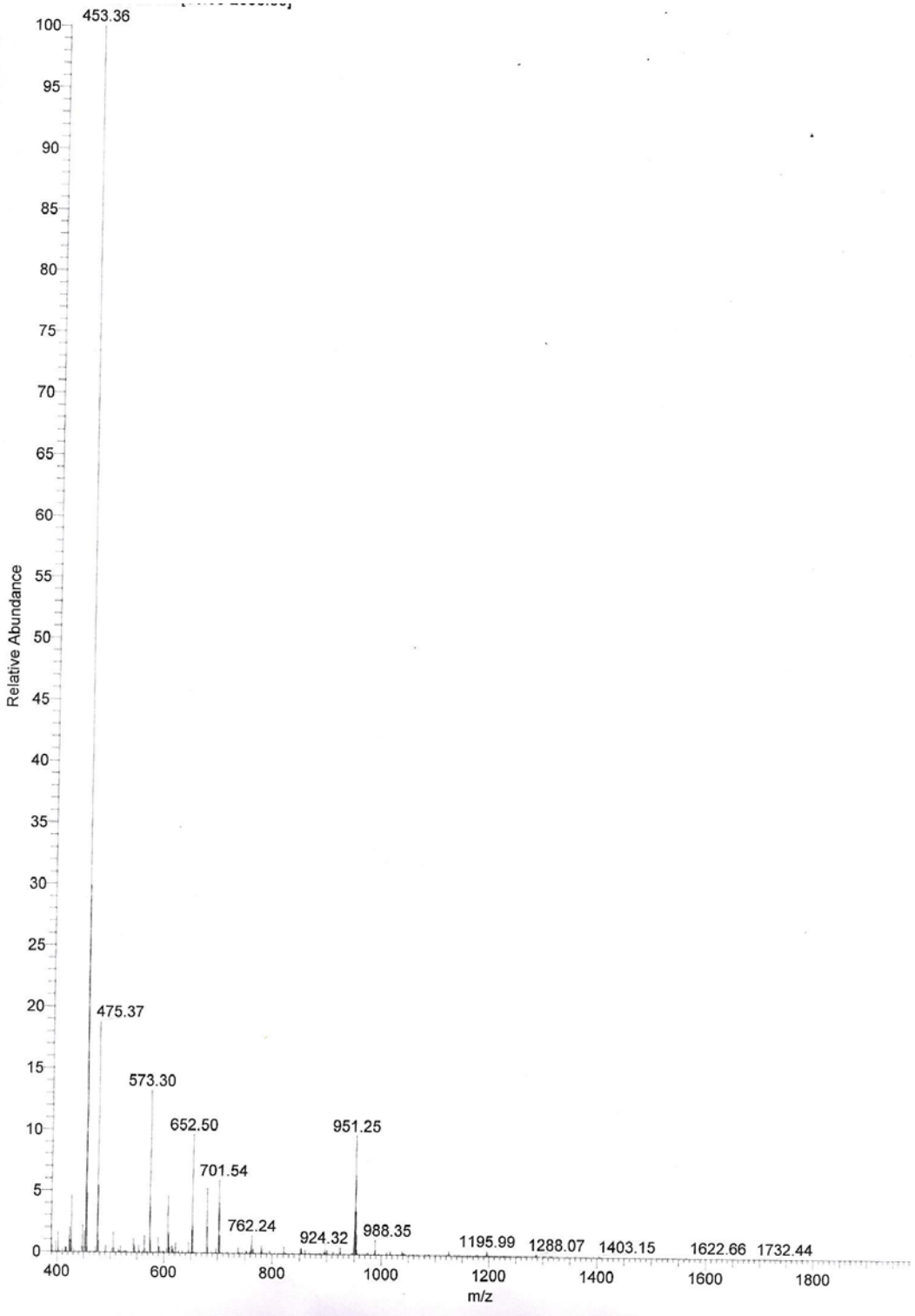

Mass spectrum for $[Cu_4(tppn)_2(FcDC)_2(H_2O)_4](ClO_4)_4 \cdot 2H_2O$

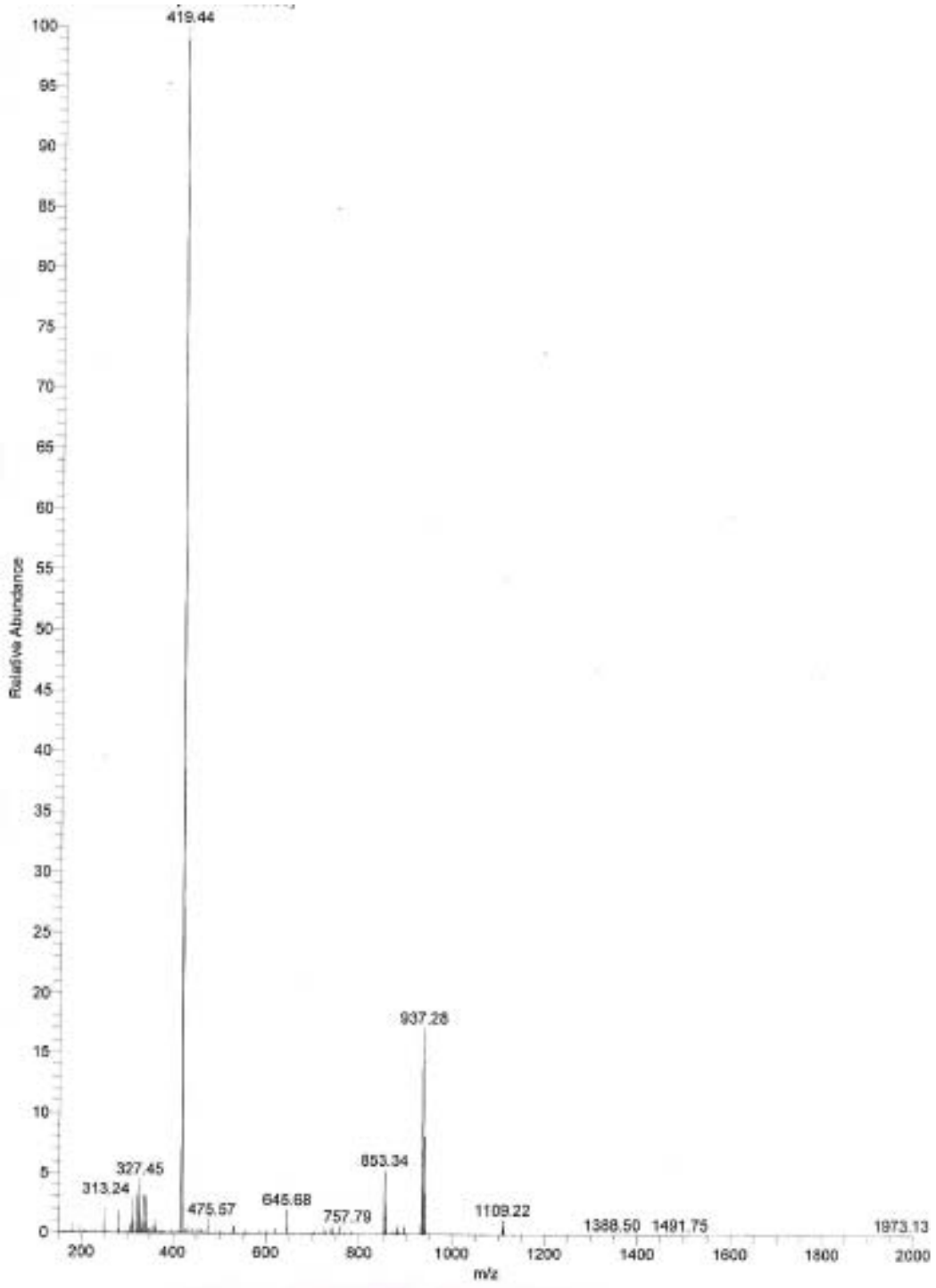

Mass spectrum for $[Cd_4(tpbn)_2(FcDC)_2(H_2O)_4](ClO_4)_4$

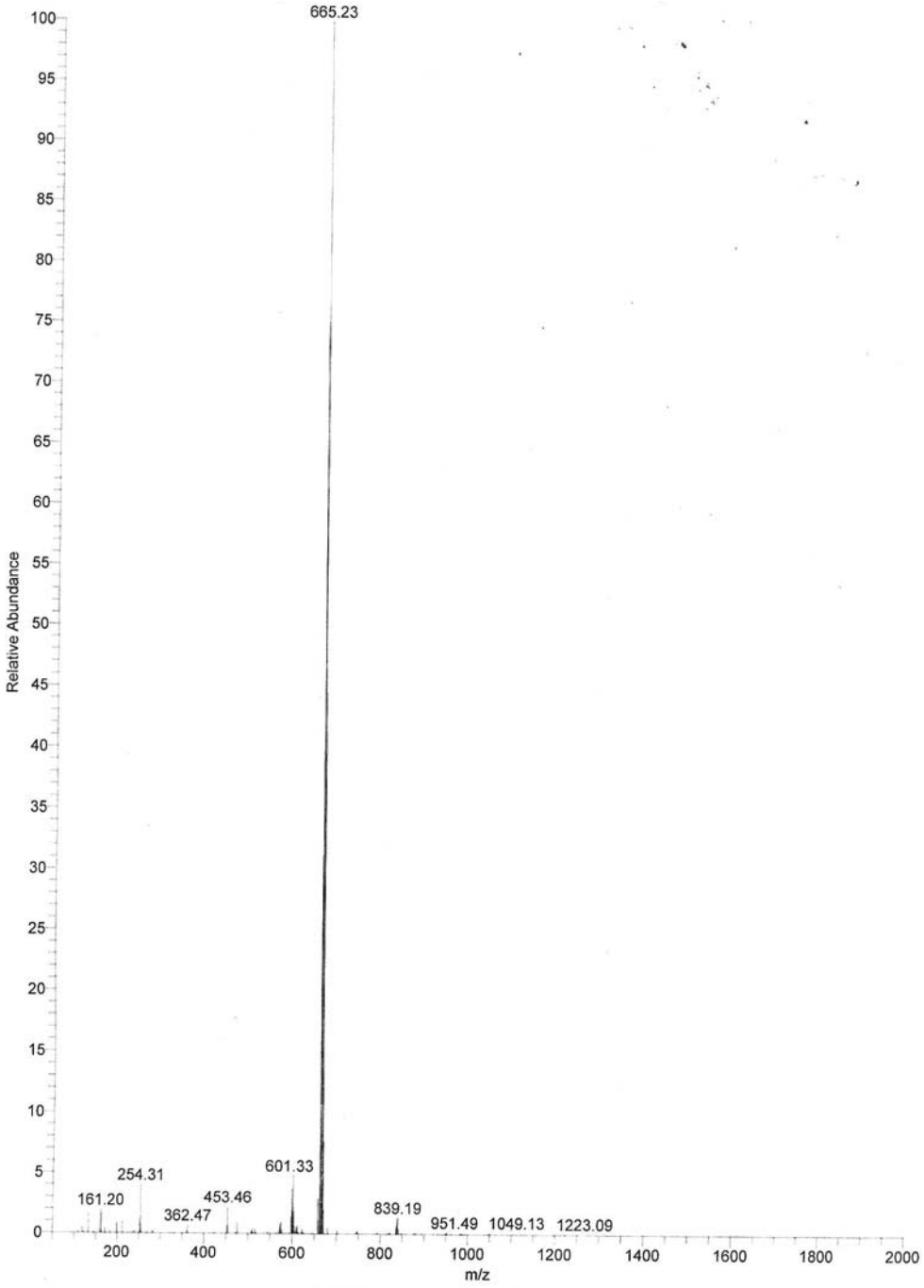

Mass spectrum for $[Cu_4(tppen)_2(FcDC)_2(H_2O)_4](ClO_4)_4 \cdot 6H_2O$

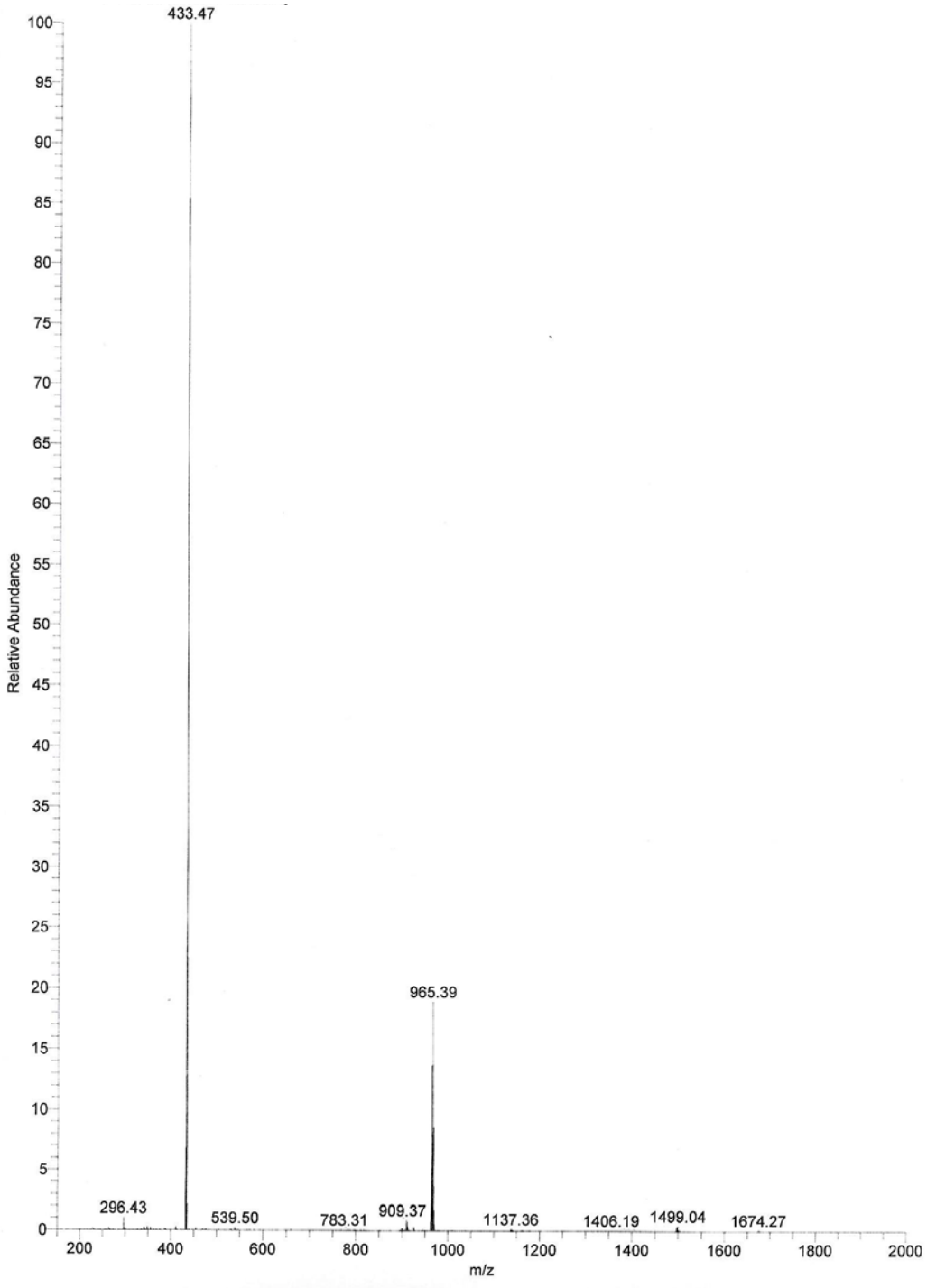

Mass spectrum for $[Mn_4(tpbn)_2(FcDC)_2(H_2O)_4](ClO_4)_4 \cdot KClO_4$